Atmos. Chem. Phys., 11, 8017–8036, 2011
www.atmos-chem-phys.net/11/8017/2011/
doi:10.5194/acp-11-8017-2011

Atmospheric Chemistry and Physics

European source and sink areas of CO_2 retrieved from Lagrangian transport model interpretation of combined O_2 and CO_2 measurements at the high alpine research station Jungfraujoch

C. Uglietti[1,2], **M. Leuenberger**[1,2], **and D. Brunner**[3]

[1]Climate and Environmental Physics, Physics Institute, University of Bern, Sidlerstr. 5, 3012 Bern, Switzerland
[2]Oeschger Centre for Climate Change Research, Zähringerstr. 25, 3012 Bern, Switzerland
[3]Empa, Swiss Federal Laboratories for Materials Science and Technology, Ueberlandstr. 129, 8600 Dübendorf, Switzerland

Received: 19 October 2010 – Published in Atmos. Chem. Phys. Discuss.: 11 January 2011
Revised: 25 May 2011 – Accepted: 3 July 2011 – Published: 8 August 2011

Abstract. The University of Bern monitors carbon dioxide (CO_2) and oxygen (O_2) at the High Altitude Research Station Jungfraujoch since the year 2000 by means of flasks sampling and since 2005 using a continuous in situ measurement system. This study investigates the transport of CO_2 and O_2 towards Jungfraujoch using backward Lagrangian Particle Dispersion Model (LPDM) simulations and utilizes CO_2 and O_2 signatures to classify air masses. By investigating the simulated transport patterns associated with distinct CO_2 concentrations it is possible to decipher different source and sink areas over Europe. The highest CO_2 concentrations, for example, were observed in winter during pollution episodes when air was transported from Northeastern Europe towards the Alps, or during south Foehn events with rapid uplift of polluted air from Northern Italy, as demonstrated in two case studies.

To study the importance of air-sea exchange for variations in O_2 concentrations at Jungfraujoch the correlation between CO_2 and APO (Atmospheric Potential Oxygen) deviations from a seasonally varying background was analyzed. Anomalously high APO concentrations were clearly associated with air masses originating from the Atlantic Ocean, whereas low APO concentrations were found in air masses advected either from the east from the Eurasian continent in summer, or from the Eastern Mediterranean in winter. Those air masses with low APO in summer were also strongly depleted in CO_2 suggesting a combination of CO_2 uptake by vegetation and O_2 uptake by dry summer soils. Other subsets of points in the APO-CO_2 scatter plot investigated with respect to air mass origin included CO_2 and APO background values and points with regular APO but anomalous CO_2 concentrations. Background values were associated with free tropospheric air masses with little contact with the boundary layer during the last few days, while high or low CO_2 concentrations reflect the various levels of influence of anthropogenic emissions and the biosphere. The pronounced cycles of CO_2 and O_2 exchanges with the biosphere and the ocean cause clusters of points and lead to a seasonal pattern.

Correspondence to: M. Leuenberger
(leuenberger@climate.unibe.ch)

1 Introduction

The present-day concentration of atmospheric carbon dioxide (CO_2) continues to rise. Ongoing emissions of CO_2 and other greenhouse gases will influence the global climate system during the next decades and centuries. It is therefore essential to gain further insight into the processes involving CO_2 exchanges among the atmosphere, the biosphere and the ocean in order to estimate the carbon sources and sinks and to comprehend the global carbon cycle. For that reason CO_2 and other atmospheric compounds are constantly monitored at several locations around the world. Long-term records obtained with high precision measurements are used to study the evolution of the changes in time and to budget the sources and sinks of atmospheric CO_2. Atmospheric oxygen observations (often measured as the ratio of oxygen to nitrogen, i.e. O_2/N_2 and expressed as $\delta O_2/N_2$ in relation to a standard ratio) can be used as a complementary carbon cycle tracer which provides additional information on the partitioning of anthropogenic CO_2 between the terrestrial biosphere and the ocean (Keeling, 1988; Keeling and Shertz, 1992; Battle et al., 2000; Van Der Laan-Luijkx et al., 2010).

Published by Copernicus Publications on behalf of the European Geosciences Union.

Systematic measurements of atmospheric O_2 have begun in 1989 by means of flask sampling at three sites (Keeling and Shertz, 1992). Since then, the flask-sampling network for atmospheric O_2 measurements has been extended over the globe (Bender et al., 2005; Manning and Keeling, 2006; Tohjima et al., 2008) and later on also included continuous on-site measurements (Manning, 2001; Kozlova et al., 2008; Valentino et al., 2008; Popa et al., 2010; Thompson et al., 2009).

The analysis of the correlation between CO_2 and O_2 is especially useful because CO_2 and O_2 are inversely coupled in terrestrial biospheric exchange processes (photosynthesis and respiration) with a rather constant stochiometric ratio of about -1.1 mol O_2 per mol CO_2 (Severinghaus, 1995). O_2 fluxes between ocean and atmosphere are mainly driven by the biological and the solubility pump, whereas ocean's CO_2 uptake is dominantly driven by the carbonate buffering system (Sabine et al., 2004). In the air-sea exchange between O_2 and CO_2 due to photosynthesis and respiration of marine biosphere (biological pump), the stochiometric ratio has been determined to be -1.4 mol O_2/mol CO_2 (Takahashi et al., 1985) clearly deviating from the terrestrial biospheric ratio. The seasonal variations in the O_2/N_2 ratio of air are partly caused by the warming and cooling of the ocean (solubility pump), also called ocean thermal effect. Typically, O_2 has a low solubility in water and exchanges very fast between the sea surface and the atmosphere with a timescale of a few weeks (Keeling et al., 1993). As oceans temperature rises in spring and summer, gases become less soluble and are transferred from the ocean to the atmosphere. In wintertime, seawater cools and the effect is reversed (Keeling and Shertz, 1992; Bender et al., 1996).The ocean is a net source of O_2 at the sea surface during spring and summer, because more organic matter is produced in the euphotic zone than is consumed by respiration. Net O_2 production begins in spring, when phytoplankton has enough light to bloom. Therefore surface seawater becomes supersaturated in O_2 and consequently a flux of O_2 towards the atmosphere is initiated which is reinforced by the thermal outgassing. Part of the organic matter produced during the phytoplankton photosynthesis accumulates in the ocean mixed layer as particulate or dissolved organic carbon (POC or DOC). In fall and winter when the sea surface temperatures cool down, the mixed layer deepens bringing O_2 under-saturated waters to the surface causing a demand of O_2 from the atmosphere and thus decreasing the atmospheric O_2 concentration. This decline continues until the following spring when a new cycle starts (Sverdrup, 1953; Siegel et al., 2002).

On the other hand, during the combustion of fossil fuels O_2 is consumed and CO_2 produced with a ratio of -1.39 mol O_2/mol CO_2. This value is the global consummation weighted average of the ratios of the different fuels, like -1.95 for gas fuels, -1.44 for liquid fuels, -1.17 for solid fuels and -1.98 for gas flaring (Marland et al., 2009). Therefore, by knowing the stochiometric ratios of O_2–CO_2 exchanges, one can separate the CO_2 uptake into land and ocean components. A sensitive tracer for oceanic air-sea gas exchange is the Atmospheric Potential Oxygen ($APO = \Delta O_2/N_2 + 1.1\Delta CO_2/0.20946$, with $\Delta CO_2 = CO_2 - 365$ ppm) as proposed by Stephens et al. (1998). Variations in APO (seasonal and latitudinal differences) are sensitive to CO_2 and O_2 air-sea exchanges plus a residual due to the fossil fuel, but APO is invariant with respect to land biospheric processes (Stephens et al., 1998).

Regarding the fossil fuel influence, our results are compared with the anthropogenic CO_2 emissions distribution in Europe according to the Emission Database for Global Atmospheric Research (EDGAR) emission inventory for the year 2005 (EDGAR v4.0, 2005, http://www.pbl.nl/en/themasites/edgar/index.html). According to the EDGAR emission map (Fig. 1), Germany (especially the Ruhr area), Belgium, the Netherlands, and Poland at the Northern side of the Alps as well as the Po valley (Northern Italy) at the Southern rim of the Alps are the major source regions of anthropogenic CO_2 in Europe. It is noteworthy that the Po valley is one of the most well-known source regions for air pollutants observed at Jungfraujoch (Reimann et al., 2004, 2008). These potential source regions are the most densely populated and industrialized countries in Europe. An exception in this regard is France due to it's high proportion of nuclear energy. The emissions per capita are highest in the Benelux states and also tend to be high in the most northern countries (heating) and Mediterranean countries (cooling systems), while emissions in the European part of Russia are only about half of those in Western Europe (Schulze et al., 2009).

In this paper, we present a record of 4.5 yr (January 2005–June 2009) of continuous measurements of CO_2 and O_2 at the High Altitude Research Station Jungfraujoch in the Swiss Alps, which is an important measurement site in Europe to monitor atmospheric composition particularly in the lower free troposphere. Our main focus is on investigating, by means of Lagrangian Particle Dispersion Model (LPDM) simulations with FLEXPART (Stohl et al., 2005), the origin of short-term deviations of CO_2 and O_2 from background concentrations at Jungfraujoch and on understanding their seasonally changing characteristics. Many studies have been carried out on local and long range transport and on identifying source and sink regions of polluted air reaching Jungfraujoch (e.g. Seibert et al., 1994, 1998; Forrer et al., 2000; Henne et al., 2005a; Cozic et al., 2008; Balzani Lööv et al., 2008; Tuszon et al., 2011). However, only few studies have done this in a systematic way using a statistical approach in which multiyear trace gas observations are interpreted by means of a large number of trajectories or LPDM results, which has the significant advantage that errors in individual transport simulations tend to cancel out. Examples for this approach are the studies by Kaiser et al. (2007) studying the origin of NO_x, O_3 and CO at several sites in the Alps and those by Balzani-Lööv et al. (2008) and

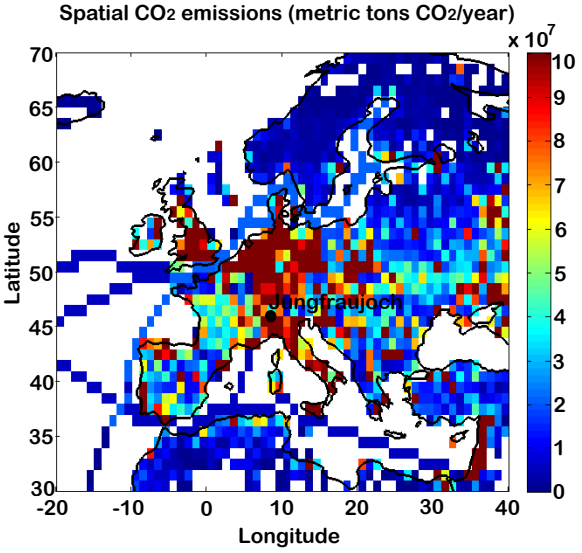

Fig. 1. EDGAR v4.0 comprises anthropogenic CO_2 emissions for the year 2005 (http://www.pbl.nl/en/themasites/edgar/index.html). The colours represent the metric tons of CO_2 emitted by the European countries per grid cell. The strategically good position of Jungfraujoch to observe European CO_2 sources is displayed as a black dot

Cui et al. (2009) investigating background concentrations and the role of stratospheric intrusions and intercontinental transport, respectively. Here, we follow such a statistical approach to classify air masses with distinct O_2 and CO_2 signatures with respect to their origin. Rather than clustering air masses according to transport histories, i.e. trajectory clustering (Moody and Galloway, 1988; Henne et al. 2008) or LPDM clustering (Paris et al., 2010; Hirdmann et al., 2010), the classification is based on identifying specific regions with the CO_2–O_2 correlation and then analyzing the air mass origin for each class. Similar to the study by Lewis et al. (2007), this approach puts more weight on the trace gas observations as compared to the transport modeling, which is likely better suited to identify different source and sink processes. However, while Lewis et al. (2007) performed an objective clustering of air masses based on simultaneous observations of multiple species, our approach is to focus on two closely interrelated species only which precluded such a cluster analysis.

2 Site description, experimental and model methods

2.1 The Jungfraujoch research station

The High Altitude Research Station Jungfraujoch (7°59′2″ E and 46°32′53″ N) is located on the Southern side of a rocky crest in the Bernese Alps, Switzerland, at an altitude of 3580 m a.s.l. (Sphinx Observatory). It is situated on a saddle between the Jungfrau peak (4158 m a.s.l.) in the west and the Mönch peak (4099 m a.s.l.) in the east. Therefore, the wind is channeled locally in north-south direction. In winter and summer more than 70 % of the wind direction is from northwest. North is also the prevailing wind direction in the other seasons.

Due to its location at high elevation and its central position in Europe the site is particularly suited to observe the free tropospheric background air above Europe (Schwikowski et al., 1995; Cozic et al., 2007; Reimann et al., 2008; Lanz et al., 2009). Nevertheless, several studies on aerosol and trace gas composition (Lugauer et al., 1998; Forrer et al., 2000; Coen et al., 2004; Reimann et al., 2004; Li et al., 2005) pointed out that Jungfraujoch is frequently influenced by direct transport from the planetary boundary layer through convection and local thermal wind systems mainly during summer, when vertical transport is more active. In addition to these rather local influences, frontal uplift of air from the European boundary layer followed by quasi-horizontal transport to Jungfraujoch episodically affects the station in all seasons of the year. Therefore greenhouse gas measurements at Jungfraujoch can capture both advected air from the polluted boundary layer as well as air from the lower free troposphere. Moreover, the permanent research station is easily accessible by railway all year round. Local emissions are usually low, since all heating is electrical and waste is transported back to the valley.

The central role of the research station Jungfraujoch is documented by the fact that it was selected as one of the Global Atmosphere Watch stations (GAW) within the framework of WMO activities. In addition, Jungfraujoch is an alpine site within the Network for the Detection of Atmospheric Composition Change (NDACC) and acts as a station within the Swiss national air pollution monitoring network (NABEL) and the European Monitoring and Evaluation Program (EMEP).

2.2 Continuous measurements of CO_2 and O_2 at Jungfraujoch

The Climate and Environmental Physics Division of the University of Bern is monitoring atmospheric CO_2 and O_2 at the High Altitude Research Station Jungfraujoch since 2000 by means of weekly flasks sampling. At the end of 2004 a continuous measurement system for in situ analysis of CO_2 and O_2 was installed in order to get an optimal data coverage to better detect short-term fluctuations in CO_2 and O_2 concentrations. Carbon dioxide is measured by a commercial NDIR infrared analyzer (S710 UNOR, SICK MAIHAK) while oxygen is measured in two ways: paramagnetically, utilizing the paramagnetic properties of oxygen molecules (at the Jungfraujoch Parox 1000 paramagnetic sensor, from MBE AG, Switzerland is used) and electrochemically, by means of fuel cells. We use Max-250 fuel cells manufactured by Maxtec, USA (Sturm, 2005; Valentino et al., 2007, 2008; Uglietti et al., 2008).

The CO_2 results are reported on the WMO mole fraction scale (XWMO 2007) whereas O_2 values are reported on our internal oxygen scale since no international and common calibration scale exists yet. The difference between the Bern internal scale and SIO scale was set to −556 per meg after measuring several times three standard air cylinders (CA07043, CA07045, CA07047) filled and determined at the Scripps Institution of Oceanography of California, La Jolla.

The continuous measurement system at Jungfraujoch is calibrated using calibration gases contained in 50 l cylinders from CARBAGAS, Switzerland. All standard cylinders are placed horizontally in order to avoid thermal and pressure fractionation of O_2/N_2. It is indeed known that for instance thermal fractionation of O_2 relative to N_2 inside high pressure gas cylinders resulting from small ambient temperature changes can lead to drifts in $\delta O_2/N_2$ values for the delivered air on the order of 10–20 per meg over the liftime of the cylinder (Keeling et al., 1998, 2004, 2005; Langenfelds et al., 2005).

Every calibration gas is passing through the entire system alternatively following an automated sequence written in LabView. We use a high CO_2 calibration gas (430 ppm), which correspond to the low O_2 calibration gas (−1300 per meg), a low CO_2 calibration gas (356 ppm) corresponding to the high O_2 calibration gas (35 per meg) and the working gas which should have CO_2 and O_2 concentrations in the range of the air sample values. The long-term reproducibility of the measurements was calculated from a standard gas which is normally measured twice a day in the same way as the sample air (every gas is measured for 6 min). Data allocation is on one second basis but the first 242 s were skipped for the data processing to avoid the abrupt transient changes occurring after the switching between different gases, whereas the next 115 s were averaged. The remaining 3 s were skipped to exclude pressure pulse influences from the valve switching. The standard error of the measurements was computed during a period of one month and the resulting reproducibility for CO_2 was determined to be less than ±0.1 ppm (around 0.06–0.08 ppm) and for O_2 to be in the range of ±8 per meg. The CO_2 value matches the target precision of 0.1 ppm. For O_2, on the other hand, the value is still higher than the target precision of 5 per meg for O_2 (Uglietti et al., 2009).

The CO_2 measurements are part of the Swiss GCOS (Global Climate Observing System) office program supporting long-term records. The online data are archived through IMECC (preliminary dataset, https://ramces.lsce.ipsl.fr/index.php?option=com_content&view=article&id=36). The CO_2 data record presented in this study have been submitted to the WDCGG database by the May 2011. The flask data are only available through the CarboEurope database.

2.3 Lagrangian transport simulations for qualitative allocation of sources and sinks

Trajectory models are a common tool in environmental and atmospheric science to study transport of air masses in the atmosphere. Trajectories describe the pathway of individual air parcels and are typically calculated based on 3-dimensional wind data from a meteorological model (Stohl et al., 1995, 1999; Stohl and Seibert, 1998). A significant shortcoming of trajectories is that they describe atmospheric transport only in a simplified way neglecting sub-grid scale turbulent and convective motions. Nevertheless, the statistical analysis of a great number of back trajectories from receptor sites has turned out to be a valuable tool to identify sources and sinks of atmospheric trace substances (Kaiser et al., 2007).

Lagrangian particle dispersion models (LPDMs) are increasingly being used in atmospheric science to study the transport and dispersion of air masses in the atmosphere (Lin et al., 2011). As opposed to simple trajectory models, LPDMs also account for turbulent motion and convection. We employed the FLEXPART LPDM (Stohl et al., 2005) in backward (receptor-oriented) mode to establish the relation between potential sources and the receptor location Jungfraujoch (Seibert and Frank, 2004). FLEXPART describes the evolution of a dispersing plume by simulating the transport of "particles", i.e. infinitesimally small elements of air, by the 3-dimensional grid-resolved wind and by sub-grid scale turbulent and convective motion. As meteorological input for the model 3-hourly fields (alternating between 6 hourly analyses and short forecasts) from operational European Centre for Medium Range Weather Forecast (ECMWF) were used. For the period January 2005 to February 2006, meteorological fields were available at $1^\circ \times ^\circ$ horizontal resolution and 60 vertical levels. In February 2006, ECMWF switched to a higher-resolution model (T799 spectral resolution, 91 levels). From February 2006 onwards, we therefore additionally prepared ECMWF input fields at much higher resolution ($0.2^\circ \times 0.2^\circ$, 91 levels) for a domain covering parts of Europe (4° W–16° E–39–51° N). This allowed us to perform nested FLEXPART simulations at high resolution over Europe and at lower resolution outside. At the coarse resolution of $1^\circ \times 1^\circ$ the ECMWF model surface at Jungfraujoch is only at 1300 m, thus more than 2 km below the true altitude. At the high resolution of $0.2^\circ \times 0.2^\circ$ the Alpine topography is better resolved and the model surface is at 2170 m. For each 3 h time interval, 50 000 particles were released from Jungfraujoch and tracked 5 days backward in time. For each simulation, a footprint was calculated which is a gridded representation of the residence time of the particles in a layer above the model surface (0–100 m in our case), and can be interpreted as a map of the sensitivity of a receptor to a source of unit strength (Seibert and Frank, 2004). Each footprint was then associated with the corresponding 3 h

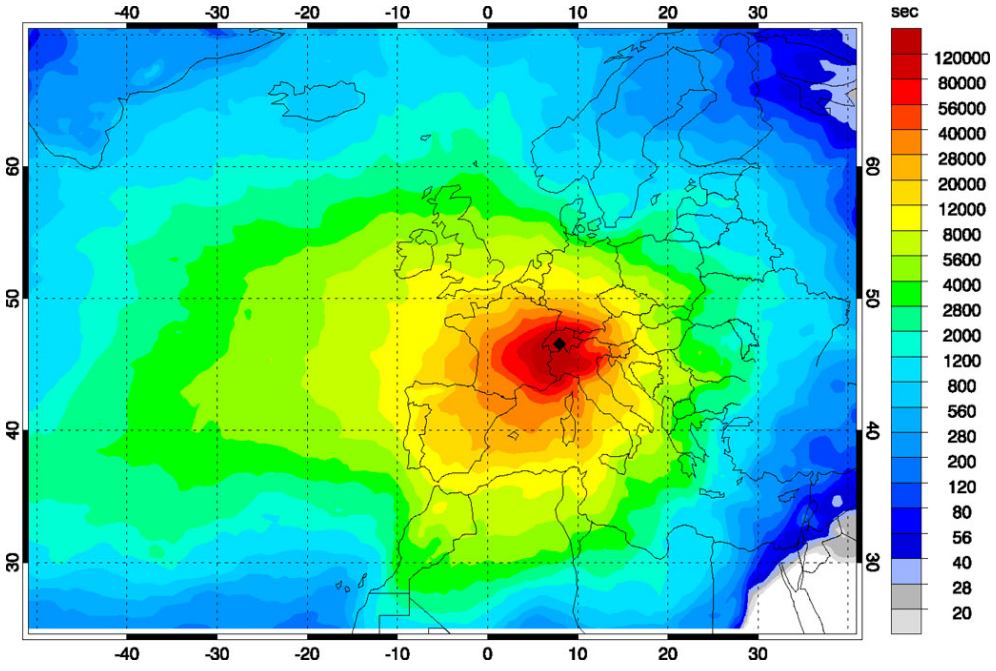

Fig. 2. Total footprint of all air masses sampled at Jungfraujoch during the investigation period (2005–2009): colour contours represent residence times of air parcels within a specific geographic grid cell relative to the maximum residence time. The maximum residence time corresponds to the end point of all trajectories, i.e. to Jungfraujoch. The lower panels show the number of trajectories per month (on the left) and per hour of the day (on the right) used to create the footprint map. Since trajectories were only calculated for valid observations, these panels demonstrate the rather uniform sampling of CO_2 over the different months of the year and hours of the day.

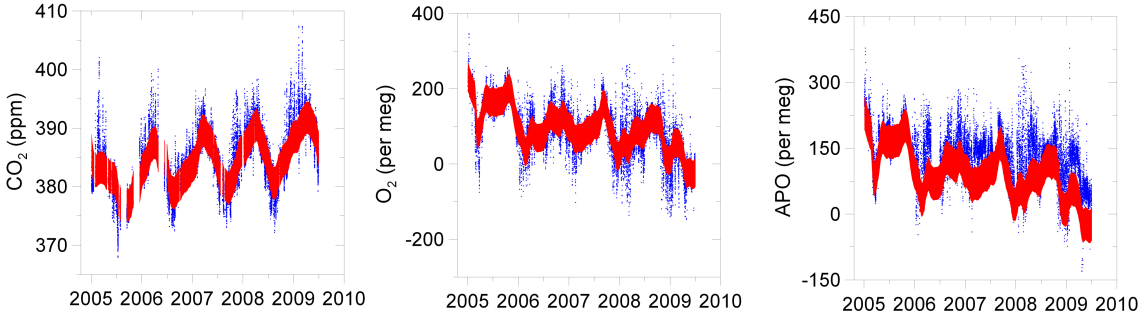

Fig. 3. CO_2 (left), O_2 (centre) and APO (right) hourly means (in blue) with the iteratively calculated background range (in red). After background subtraction, the remaining data is considered and included in the Lagrangian transport simulation.

average of the CO_2 and O_2 measurements. Particles were released from 3000m which is a compromise between the model surface altitude and the real station height and is based on a comparison of specific humidity measurements at Jungfraujoch with vertical profiles acquired from routinely launched soundings in Payerne over the flat Swiss Plateau (46.8° N and 6.9° E), which showed best agreement around 3000 m. The best release altitude for mountain stations is a matter of ongoing debate. In the study of Folini et al. (2008), for example, the best results were obtained for particles released from Jungfraujoch close to the model surface. However, their results, which were based on a different LPDM and simulations at higher resolution using a mesoscale model, are not directly applicable here. Since our study focuses on qualitative assessment of source/sink regions rather than on quantitative emission estimation, we do not consider the choice of release altitude as being critical. It should also be noted that the first version of our manuscript (Uglietti et al., 2011) has been based on trajectory calculations at lower resolution in which the model surface at Jungfraujoch was more than 800 m lower than in the present simulations. Nevertheless, the results had been quite similar.

The total footprint, i.e. the sum of all footprints from January 2005 to June 2009 is presented in Fig. 2. Not surprisingly, the influence from the western direction is enhanced in comparison to the east due to the prevailing westerly winds (Reimann et al., 2008). The maximum residence time and thus the maximum sensitivity to source/sink processes is close to the receptor point Jungfraujoch and decreases rapidly with increasing distance (approx. with the squared distance). The footprints also help to understand the general pattern of atmospheric transport to Jungfraujoch. Air masses from the PBL are typically transported to the site by meteorological processes generating substantial upward motion such as fronts, Foehn events or thermal up-lifting by convection during anticyclonic periods in summer. These events together with associated atmospheric tracer concentrations can be used to assess emission areas from the European continent.

Transport patterns and source/sink regions associated with air masses with distinct CO_2 and O_2 characteristics (e.g. very high CO_2 levels during anthropogenic pollution episodes) are visualized in this study by means of "relative footprints". These are obtained by dividing the total footprint of a given set of observations with concentrations above or below a threshold by the overall total footprint shown in Fig. 2, after first scaling both footprints by the respective number of data points. The relative footprint is directly proportional to the Potential Source Contribution Function (PSCF) proposed in other studies (Zeng and Hopke, 1989; Scheifinger and Kaiser, 2007) in which this concept was applied to trajectory rather than LPDM simulations. The only difference is the scaling by the number of footprints (or trajectories) which makes the relative footprint independent of the number of points selected in a given subset. The relative footprint indicates where a selected subset of air masses has spent relatively more (or less) time close to the surface than the "average air mass" observed at Jungfraujoch. The strong radial pattern of absolute footprints with a peak at Jungfraujoch as seen in Fig. 2 is eliminated by the use of relative footprints or PSCF (Scheifinger and Kaiser, 2007).

3 Results

3.1 CO_2 and O_2 time series

Hourly means of CO_2 and O_2 online records from Jungfraujoch are presented in Fig. 3 and the corresponding mean seasonal cycles in Fig. 4. Atmospheric oxygen and carbon dioxide reveal the typical behaviour observed at mid-latitude sites of the Northern Hemisphere. The CO_2 winter maximum is reached in March, when the photosynthetic sink sets in to take up CO_2 and to release O_2. Then the CO_2 mixing ratios decline rapidly during the May–July growing season and reaching a minimum in August. Afterwards, the CO_2 level rises slowly during September–November because of ecosystem respiration and approaches the maximum to start the seasonal cycle again. O_2 is not exactly six-months out of phase with CO_2. It reaches maximal values in the period end of August until the beginning of September (one months later than the CO_2 minimum) and minimal ones in March. This offset in timing of seasonal extremes between CO_2 and O_2 is due to the ocean that affects O_2 stronger than CO_2. Thermal CO_2 outgassing is opposite in sign to the marine photosynthesis and respiration CO_2 flux thus leading to only a small seasonal variation in CO_2 air-sea exchange in addition to the dampening effect of the ocean's carbonate chemistry.

On the contrary, the thermal effect and the biological activity act synchronously for the O_2 air-sea exchange, reinforcing the O_2 seasonal cycle (Keeling and Shertz, 1992; Bender et al., 1996). Moreover the O_2 air-sea exchange takes place on shorter times (few weeks) compared to the CO_2 air-sea exchange (1 yr) (Keeling et al., 1993).

The CO_2 and O_2 time series at Jungfraujoch can be separated in three components: first the long term trend covering variations on timescales of years to decades. Second, the mean seasonal component which represents the variations related to the biospheric cycle of photosynthesis and respiration and to a lesser extent to marine CO_2 and O_2 exchanges. Finally a short term component including hourly to weekly variations mainly associated with meteorological variability and corresponding shifts in transport patterns.

3.2 Background corrected data

Since our LPDM simulations only account for the recent history (past five days) of the air measured at Jungfraujoch a background corrected record is calculated. The background was computed using an iterative procedure: 30 days running

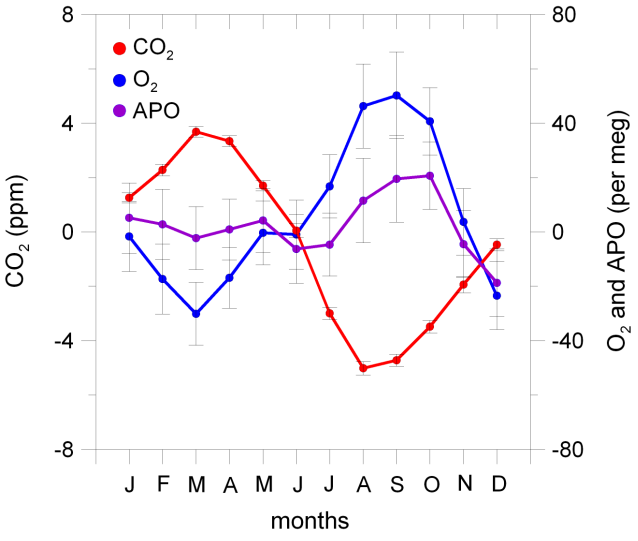

Fig. 4. Seasonal cycle of CO_2 (red curve), O_2 (blue curve) and APO (purple curve) at Jungfraujoch expressed as deviation from the mean concentration. The seasonal cycle of O_2 is approximately six months out of phase with the CO_2 cycle. APO is slightly decreasing from January until June followed by a maximum in autumn. Error bars are the measurement uncertainties.

means and their standard deviations were calculated. All data points above and below 2σ (red band in Fig. 3) were then rejected and the procedure was repeated until convergence (in particular 26 % of CO_2 values and 32 % of O_2 values were rejected). The resulting background was then subtracted from the original data producing the background subtracted records of CO_2, O_2 and APO as shown in Fig. 5. This record represents the third, short-term, component of variability mentioned above, and is used in the following to identify the source and sink regions of CO_2 and O_2 for high frequency anomalies.

3.3 Seasonal cycle

The mean seasonal cycle for the Jungfraujoch in situ measurements (displayed in Fig. 4) was derived from the background data by subtracting first the long-term trend (for every background value the corresponding trend value was subtracted). The trend was calculated according to the method of Nakazawa et al. (1997), using a smoothing cubic spline as stated also in Valentino et al. (2008) and Uglietti et al. (2008). The resulting values were then averaged over the monthly means of the different years (Morimoto et al., 2003). The difference between the CO_2 summer minimum and the winter maximum (seasonal amplitude) is 8.7 ± 0.2 ppm, while the opposite variation in the O_2 signal is 80 ± 13 per meg and in APO 23 ± 15 per meg, respectively. These amplitudes are smaller compared to other sites in Europe (CarboEurope atmospheric measurement sites) because Jungfraujoch is at a high altitude where the dilution effect plays an important role, diminishing the amplitude. Moreover Jungfraujoch is less influenced by the terrestrial biosphere (especially areas covered by forests) compared to the other remote sites in Europe (i.e. tall towers).

3.4 Long term and short term variations

The trends were calculated first by subtracting the mean seasonal cycle (a fit curve with two harmonics was computed as seasonal cycle by means of the method described by Nakazawa et al., 1997) from the observations and then computing the linear trend for every year. The online record (Fig. 3) is relatively short in time (January 2005–June 2009) to draw conclusive statements about the long term trend. Nevertheless we calculated a mean annual CO_2 growth rate, by computing the linear trends year by year and not using the smoothing cubic spline as for the entire trend line. The resulting mean annual CO_2 growth rate corresponds to $1.89\,\mathrm{ppm\,yr^{-1}}$ which is in agreement with the global growth rate ($1.91\,\mathrm{ppm\,yr^{-1}}$) calculated by the IPCC for the decade 1995 to 2005 (Forster et al., 2007). Our investigations focussed on the short-term variations as displayed in Fig. 5. In the following section, model experiments are presented for data interpretation of classified short-term variations based on a CO_2 and O_2, or APO.

4 Model experiments

In order to better understand the daily to weekly CO_2 and O_2 variations with regard to their underlying processes and source areas, it is helpful to cross-plot them as done in Fig. 6 (O_2 versus CO_2 (left) and APO versus CO_2 (right)). In the following we focus on the interpretation of specific subsets of points in the scatter diagram: extreme events of high CO_2 are first investigated in Sect. 4.1 in the form of case studies. A more statistical analysis is then presented in Sect. 4.2 for large clustered subsets of APO versus CO_2. In each case the interpretation of the data is supported by an analysis of air mass origin by means of relative footprint maps.

4.1 Extreme events of high CO_2

A number of particularly high CO_2 concentrations (>10 ppm above average) were recorded at Jungfraujoch as documented in Fig. 5. In the following we focus on two high CO_2 concentration events showing very different relative footprints.

4.1.1 Case 1

The first was observed in the period from 24 to 27 February 2005. According to the in situ measurements CO_2 concentrations began to increase in the morning of 24 February reaching a maximum of 395.75 ppm at around 21:00 UTC and decreased from the morning of 25 February.

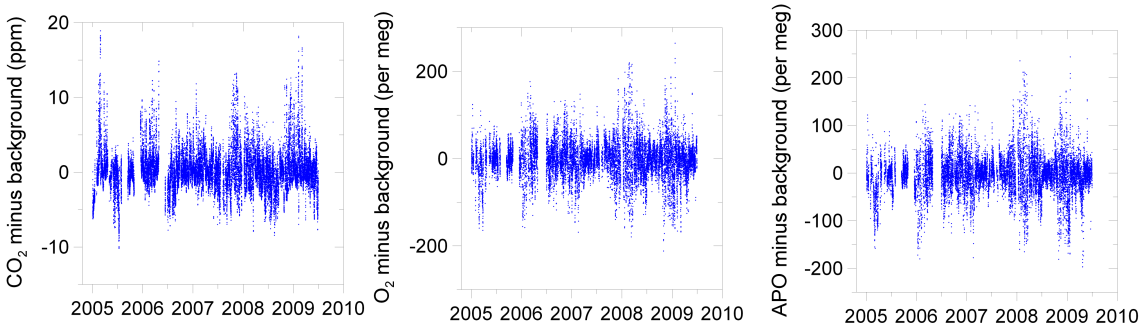

Fig. 5. CO_2 (left), O_2 (center) and APO (right) records after background subtraction.

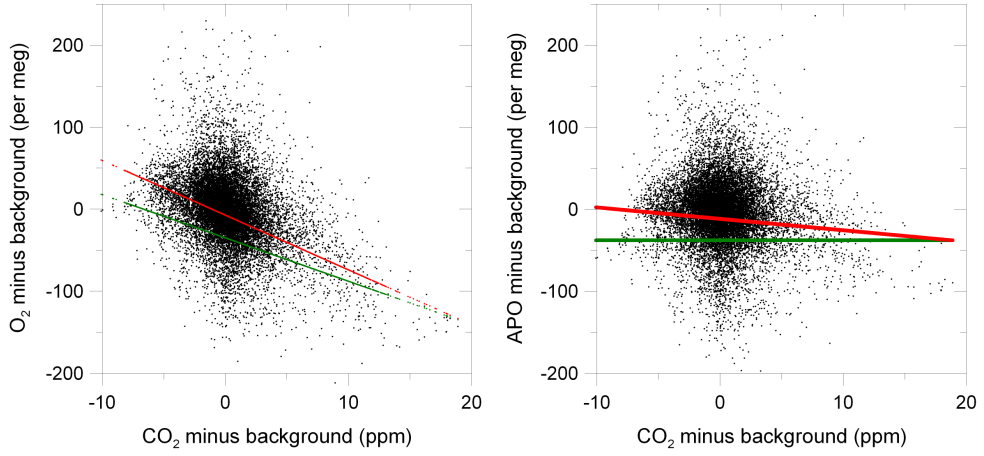

Fig. 6. Scatter plot of O_2 versus CO_2 (left) and of APO versus CO_2 (right). Both records are background corrected. The slopes of fossil fuel burning (-1.4 mol mol^{-1}, red line) and of land photosynthesis and respiration (-1.1 mol mol^{-1}, green line) are overlaid for reference. APO is invariant with respect to land biospheric processes by its definition (green line, right panel).

Then the concentration increased a second time during 27 and 28 February, reaching a maximum concentration of 402.01 ppm. On 25 February the flasks sampling procedure took place in the morning between 06:45 and 07:00 and the mean CO_2 concentration measured afterwards at the University of Bern by mass spectrometry was 393.41 ppm.

The analysis of Black Carbon (BC) at Jungfraujoch, performed by the Laboratory of Atmospheric Chemistry of the Paul Scherrer Institute (PSI), shows a peak of 550.25 ng m^{-3} on 24 February and another peak of 542.91 ng m^{-3} on 27 February (data available at EBAS Database, http://ebas.nilu.no).

Generally, carbonaceous aerosols (BC) are emitted by incomplete combustion processes such as fossil fuel combustion, wood burning, charcoal combustion or natural fires (Stoffyn et al., 1997; Castro et al., 1999). As reported in previous studies (Baltensperger et al., 1991; Petzold et al., 2007) occasionally large aerosol and BC peaks attributed to long-range transport events (e.g. forest fires) occur at Jungfraujoch. In general BC concentrations at Jungfraujoch exhibit a seasonal cycle with lower values in winter and a maximum in summer, due to the injection of air from the more polluted planetary boundary layer during summertime (Weingartner et al., 1999; Henne et al., 2005b).

In the framework of the GAW aerosol monitoring program several measurement campaigns have been conducted at Jungfraujoch in the period 2004–2005 to characterize the physical and chemical properties of tropospheric aerosols. On 25 February the concentrations of the chemical species analyzed (sulfate, nitrate, ammonium, organic matter, BC) were exceptionally high for the winter season and more reminiscent to typical summer values (Cozic et al., 2008).

The relative footprint map (Fig. 7) for the considered period shows high residence time of air masses above Eastern Europe and Germany. Actually MeteoSwiss reported for that period an unusual phase of cold weather conditions with repeated surges of arctic air hitting the Alps associated with light snowfall recorded at several weather stations on the Northern side of the Alps. The Southern side of the Alps was protected from these cold fronts and experienced almost no precipitation (Bader and Schlegel, 2005). This persistent weather situation appears to have induced large accumulation

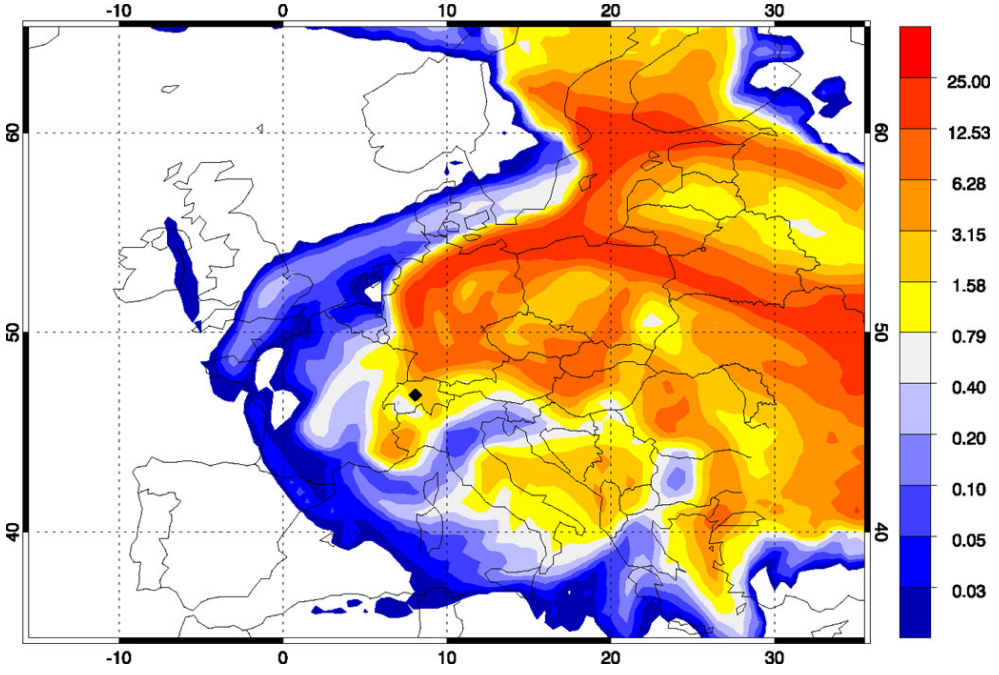

Fig. 7. Relative footprint map of trajectories associated with exceptionally high CO_2 concentrations (extreme event, case 1) recorded with the continuous measurements system at Jungfraujoch between 24 and 27 February 2005. Air masses originate from northeastern Europe. Colors correspond to the ratio of residence times over specific grid-cells relative to the average residence time of all trajectories, with yellow to red colors indicating above average and blue colors below average residence times. E.g. a value of 10 denotes that the selected trajectories had a 10 times higher probability to have passed over a particular grid cell than any arbitrary trajectory released from Jungfraujoch

of trace gases in these air masses as they moved from the north passing over heavily industrialized countries before they were lifted by the frontal activity and finally transported to Jungfraujoch.

4.1.2 Case 2

The second high concentration event discussed here occurred between 21 and 24 November 2007. Also in this case the high values were recorded with both techniques, i.e. the continuous measurement system and the flask sampling. The maximum concentration, recorded in the morning of 23 November around 08:00 UTC, was 397.4 ppm. The concentration started to increase during the afternoon of 21 November and returned to the mean concentration of 384 ppm in the morning of 24 November.

The corresponding relative footprint (Fig. 8, left) shows air masses originating from the Atlantic Ocean and North Africa and passing with high residence times over the Mediterranean Sea. Nevertheless vertical transport to Jungfraujoch during south Foehn events, which is typically associated with precipitation and convection along the southern flank of the Alps, is not well resolved by the ECMWF model at the coarse resolution of only $1°\times1°$ as used here. We therefore also analyzed trajectories based on much higher resolution (7 km×7 km) wind fields of the COSMO model of MeteoSwiss for this day. They reveal rapid vertical ascent from the Po Valley and the Italian peninsula within only one day before reaching Jungfraujoch (not shown).

The high CO_2 concentrations recorded for these days were also associated with relatively high CO values (as observed by the NABEL network). These high trace gas concentrations could be explained by advection from the Po valley due to a typical south Foehn event. However, air reaching measurement sites at the Northern edge of the Alps often originates from altitudes of about 2000 m a.s.l. in the south and not necessarily from low altitude in the boundary layer (Seibert, 1990; Campana et al., 2005). Consequently, there are south Foehn events which transport highly polluted air from the Po Basin to the Jungfraujoch and others with no sign of pollution when the origin was probably above the boundary layer (Campana et al., 2005).

In this study case it is very likely that the high CO_2 concentrations are caused by contact of these air masses with polluted air above the Po valley before arriving at the Jungfraujoch (Forrer et al., 2000).

Indeed Meteo Swiss (Fig. 8, right) reported for those days (21–23 November 2007) the formation of a depression over the Bay of Biscay which has sparked an inflow from the southwest and south with the addition of moist air into the Southern rim of the Alps. This has established a classical Foehn situation with substantial precipitation amounts on the

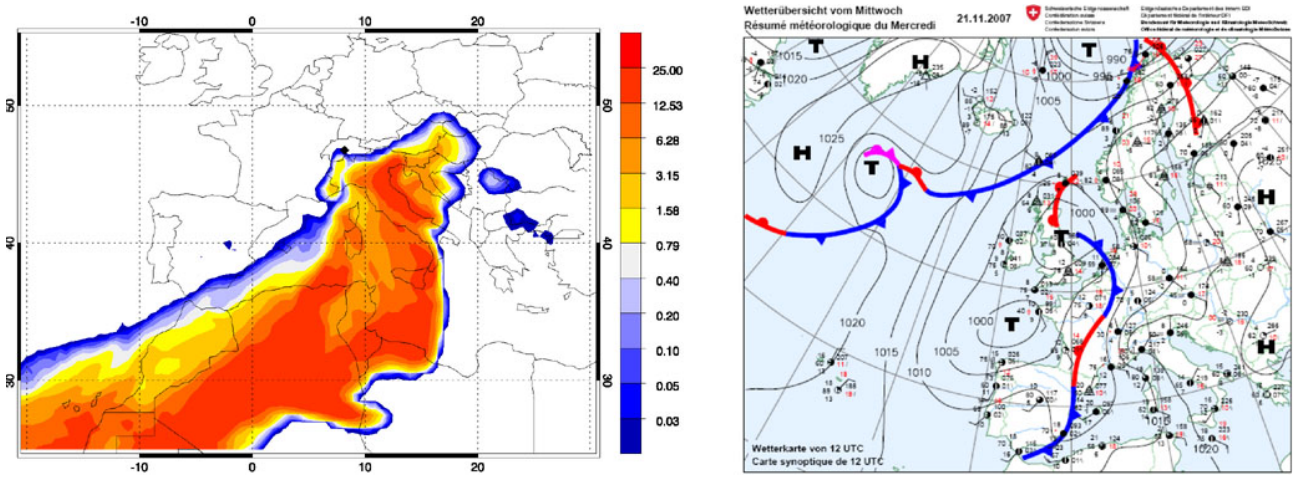

Fig. 8. Relative footprint map of trajectories corresponding to high CO_2 concentration (extreme event, case 2) measured on 23 November 2007 (left). See Fig. 7 for explanation of the color legend. South Foehn situation on 21 November (right) as represented in the daily surface weather analysis of MeteoSwiss (available from http://www.meteoschweiz.admin.ch/web/de/wetter/wetterrueckblick.html)

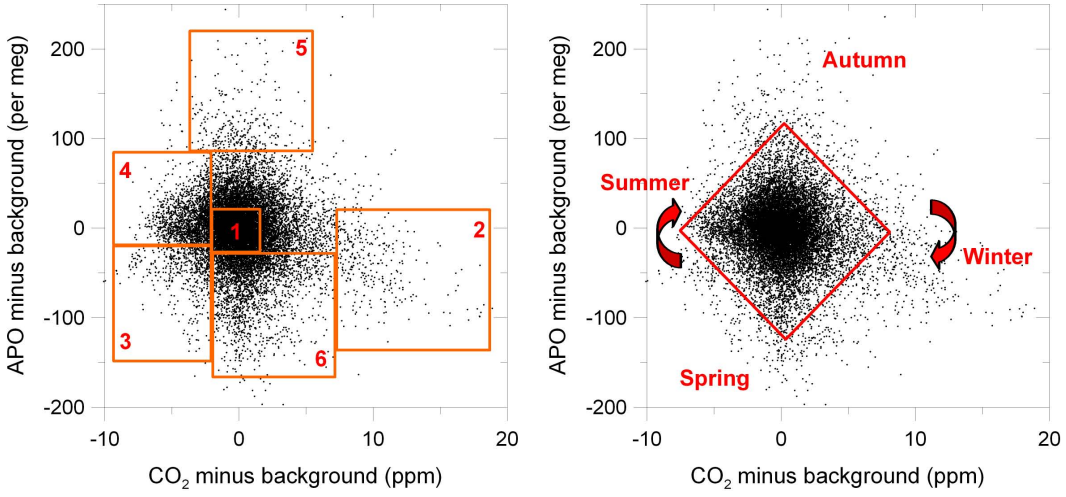

Fig. 9. Different selections (see text for explanations) in the scatter plot of the background corrected APO versus background corrected CO_2 (left panel). Seasonal cycle of defined subsets (right panel).

Southern side of the Alps (Bader and Croci-Maspoli, 2007). Moreover the analysis of wind speed and directions recorded at Jungfraujoch by Meteo Swiss confirms the south flow showing that the wind direction changed abruptly on the 18 from north to south until 25 of November, when the wind direction changed back to north.

In contrast to case 1 the BC measurements at Jungfraujoch did not show any anomalous values during this event. It is likely that, in contrast to CO_2 and CO, the aerosols have been washed out by precipitation. This increase of CO_2 without a simultaneous increase of BC may thus be interpreted as a typical indicator of south Foehn events because during such events aerosols tend to be washed out by precipitation.

4.2 Origin of air masses for different CO_2 and APO concentrations subsets

This section investigates the influence of different air mass origins on CO_2 and O_2 concentrations at Jungfraujoch in a more statistical way, by analyzing the combined footprints of a a large number of observations corresponding to specific subsets of points in the APO-CO_2 scatter plot. Each subset is represented by a certain range of CO_2 and APO values. Note that the advantage of using APO instead of O_2 is due to the definition of APO that guarantees a subtraction of a mean terrestrial biosphere influence and therefore allows a better distinction of ocean and terrestrial biosphere influences on CO_2 than CO_2 vs. O_2.

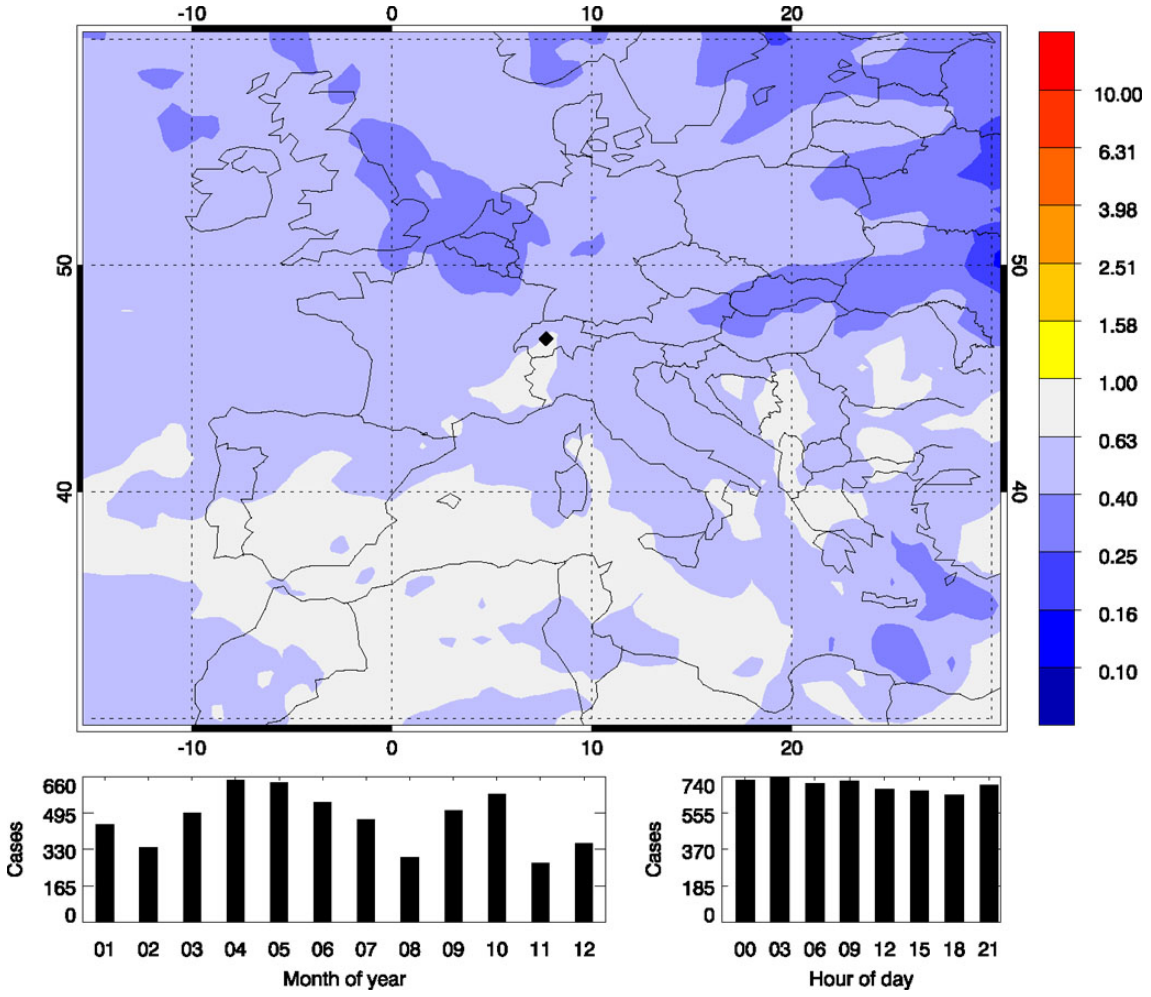

Fig. 10. Relative footprint map of trajectories associated with background values of CO_2 and O_2 recorded at Jungfraujoch (background calculated as explained in Sect. 3.1) See Fig. 7 for explanation of the color legend. The lower panels show the number of trajectories that were released in a specific month (left) and in a specific period of the day (right).

The selection of subsets is illustrated in Fig. 9, left panel. We only select subsets of points with outstanding characteristics. The selection is somewhat subjective, and it is a compromise between representing clear (outstanding) signals in trace gas concentrations and including a sufficiently large number of points to obtain robust patterns in the corresponding trajectory footprints.

The box in the middle (Fig. 9, left panel, subset 1) corresponds to background values. All points are within the 2σ bands of CO_2 (± 2.71 ppm) as shown in Fig. 3 (red band) and APO (± 37 per meg). The other five subsets are defined as follows: points with enhanced CO_2 and reduced APO (Fig. 9, left panel, subset 2); points with low CO_2 and low APO (subset 3); points with low CO_2 but enhanced APO (subset 4); points with high APO but normal CO_2 (subset 5); points with regular CO_2 and low APO (subset 6). In the following all selected subsets defined above are discussed. The occurrence of specific subsets follows a seasonal cycle as indicated in Fig. 9, right panel. Air masses enhanced in CO_2 are preferentially observed in winter, those depleted in CO_2 in summer. Associated with the seasonal cycle in air-sea exchange is a seasonal cycle in APO with a tendency of negative anomalies occurring in spring and positive anomalies in autumn. The fraction of points per subset is: Subset 1: 62 %; Subset 2: 2.0 %; Subset 3: 2.9 % (1.7 % if restricted to summer months); Subset 4: 8.9 %; Subset 5: 1.7 %; Subset 6: 11.6 %. Remaining points not belonging to a subset: 11 %. Quite a large fraction is thus in the background cluster, which is actually explaining that that most of the time the Jungfraujoch observes undisturbed background air.

4.2.1 The background cluster (subset 1)

By applying the back trajectories analysis to background values (all data within $\pm 2\sigma$), the relative footprint map shown in Fig. 10 is obtained. Values below 1 dominate

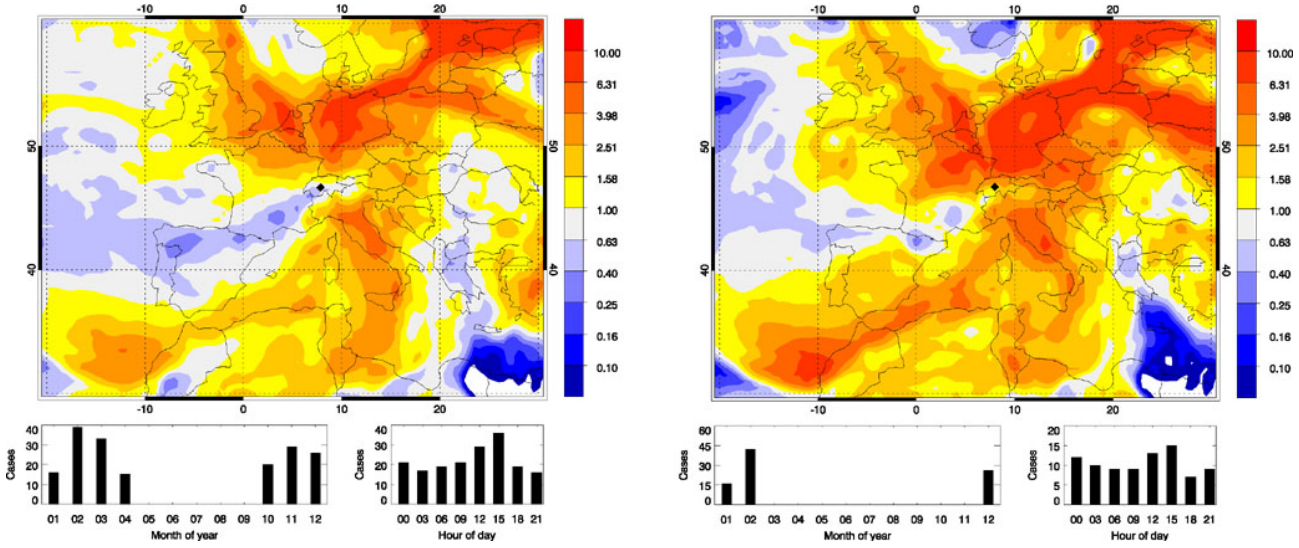

Fig. 11. Relative footprint maps for the situation with high CO_2 and low O_2 (subset 2). The left panel represents the relative footprint map for year round values whereas the right panel shows the winter only selection. The trajectories are mainly coming from Northeastern Europe with increased residence times over Northern Germany and Eastern European Countries (yellowish and reddish colours) See Fig. 10 for further details.

(blue colours), indicating that these air masses had less than average contact with the European boundary layer. This is expected for background values and demonstrates the success of the classification based on FLEXPART simulations for this class. There seem to be somewhat more air masses classified as background in both spring and autumn (mainly October), possibly because these are transition seasons for the biosphere with neither large emissions nor uptake. There is also a north-south gradient as documented by the colours. Background air masses from the north tend to have been even less in contact with the PBL than those from the south. This is understandable from a meteorological point of view since advection of background air from the north is typically associated with anticyclonic flow and therefore subsidence. Such conditions appear to be ideal to observe undisturbed free tropospheric air.

4.2.2 Enhanced CO_2 and reduced APO and O_2 (subset 2)

The high CO_2 and low O_2 concentrations recorded at Jungfraujoch occur generally in wintertime because of increases due to the lower biospheric activity (more O_2 is used for respiration) and higher anthropogenic CO_2 emissions in Europe due to the burning of different fossil fuels (solid, liquid or gas) (Rotty, 1987), thus enhancing the decrease of atmospheric oxygen. In wintertime the boundary layer is mostly located below the altitude of Jungfraujoch and the high CO_2 concentrations cannot be explained by thermal uplift of polluted air masses from the valleys surrounding Jungfraujoch. These high concentrations are thus likely associated with air masses which had resided in the polluted boundary layer for extended periods of time and were then transported to the free troposphere probably in connection with frontal activity. The left panel of Fig. 11 represents all CO_2 pollution events which mostly but not exclusively occurred between October and April. Since the near-surface residence time of air masses reaching Jungfraujoch is generally about 26 % lower in winter than in summer a winter only map was calculated (Fig. 11, right) in which the total wintertime footprint served as reference for the computation of the relative footprint. This figure emphasizes the enhanced residence times of these air masses over the eastern parts of Europe (Poland and Germany). Thus the high CO_2 concentrations may be explained by the passage of air masses above polluted areas in those countries. Therefore, from the EDGAR emission map (Fig. 1) these areas can be considered as potential source regions for polluted air masses reaching Jungfraujoch. The elongated, curved patterns of enhanced residence times (yellow to red areas in Fig. 11, right) suggest that transport associated with such events typically followed a cyclonic path supporting the hypothesis of the importance of frontal lifting. In both case studies presented earlier, the upward transport to Jungfraujoch was indeed connected with fronts.

4.2.3 Low CO_2 and low APO (subset 3)

Air masses with low CO_2 and comparatively low O_2 are almost exclusively observed in summer and describe air masses advected from Eastern Europe (Fig. 12).

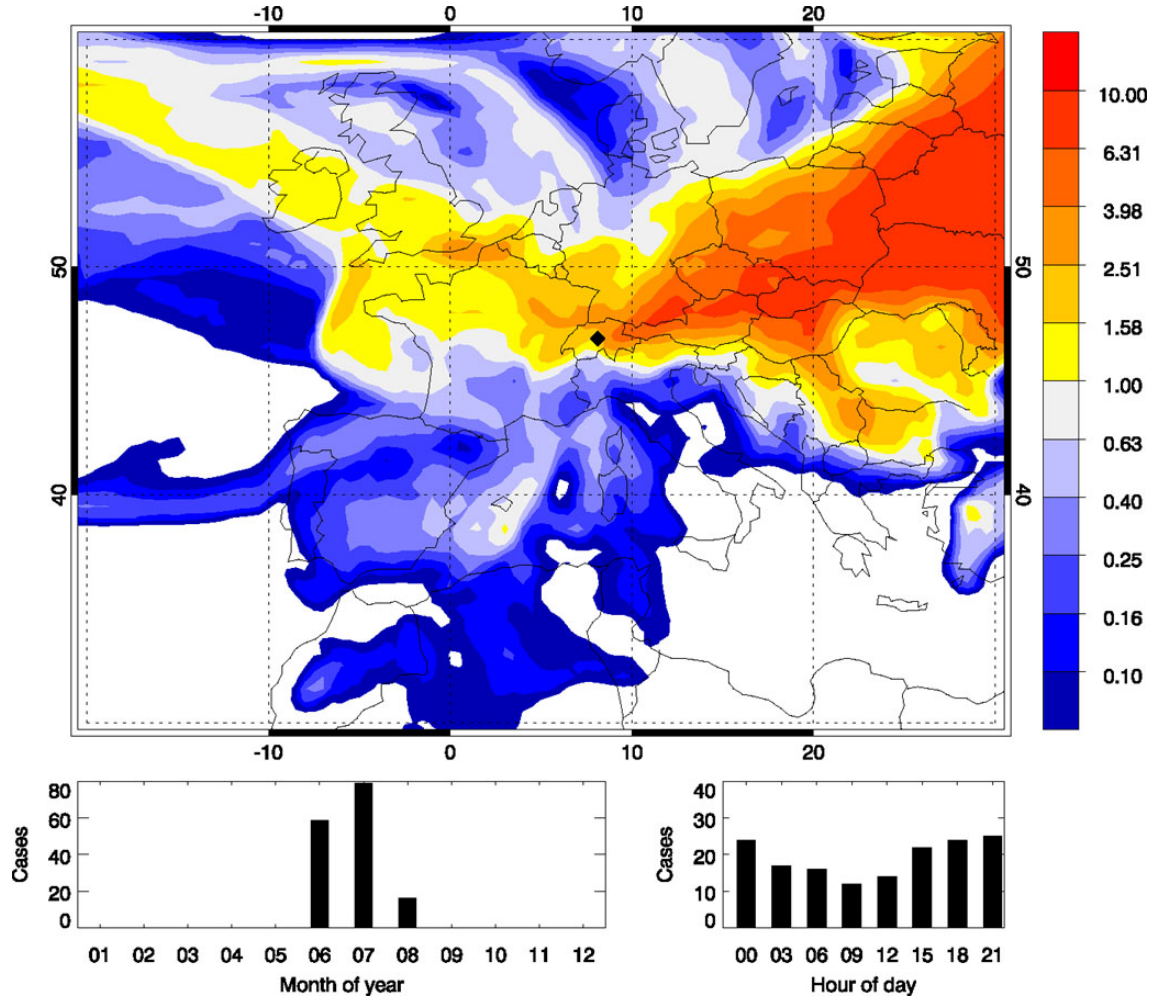

Fig. 12. Relative footprint map associated with low CO_2 and low O_2 and APO concentrations (subset 3). See Fig. 10 for further details.

The low CO_2 concentration is an effect of plant CO_2 uptake, but O_2 in these air masses is not enhanced as would be expected from photosynthesis. Therefore, a strong oxygen sink is needed. To our knowledge four options may be considered for this sink: (i) fossil fuel consumption, (ii) stratosphere-troposphere exchange (STE), (iii) atmosphere-ocean exchange and (iv) oxidation of soil organic material. Option (i) is rated as improbable considering that the percentage of fossil fuel emissions (Fig. 1) compared to the natural carbon exchange is low its influence on the oxygen budget is limited despite the higher carbon oxidation ratio (-1.39 mol O_2/mol CO_2). To option (ii), it has recently been reported that O_2/N_2 ratios are enriched with increasing altitude (Ishidoya et al., 2008) associated with decreased CO_2 concentrations (Gurk et al., 2008). This behaviour is explained by altitude dependent air age. Hence a reduced STE would lead to an apparent O_2 sink and CO_2 source due to delayed upward transport of ground-based emission signals. If this option would be the major cause then ozone measured at Jungfraujoch should express lower values as reaction to this STE reduction, yet ozone shows a summer maximum. Therefore, this option seems also improbable. Option (iii): Atmosphere-ocean exchange is important for atmospheric O_2 concentrations. In summer, however, we would expect increased outgassing from the ocean due the increased temperature. This is exactly opposite (neglecting the marine biosphere activity) to what is needed. Furthermore, air masses for subset 3 are dominantly originating over the continent with an actively growing biosphere (low CO_2, high O_2). Yet, a slight timing difference of the temperature induced ocean source for O_2 in summer compared to the terrestrial biosphere O_2 source could lead to an ocean-continent gradient. The observed low CO_2, O_2 and APO values for subset 3 might be the result of such a gradient with advected air masses from the continent that have not been in contact with the ocean surface for an extended period of time (weeks) and therefore have O_2 (APO) values which are lagging behind the normal

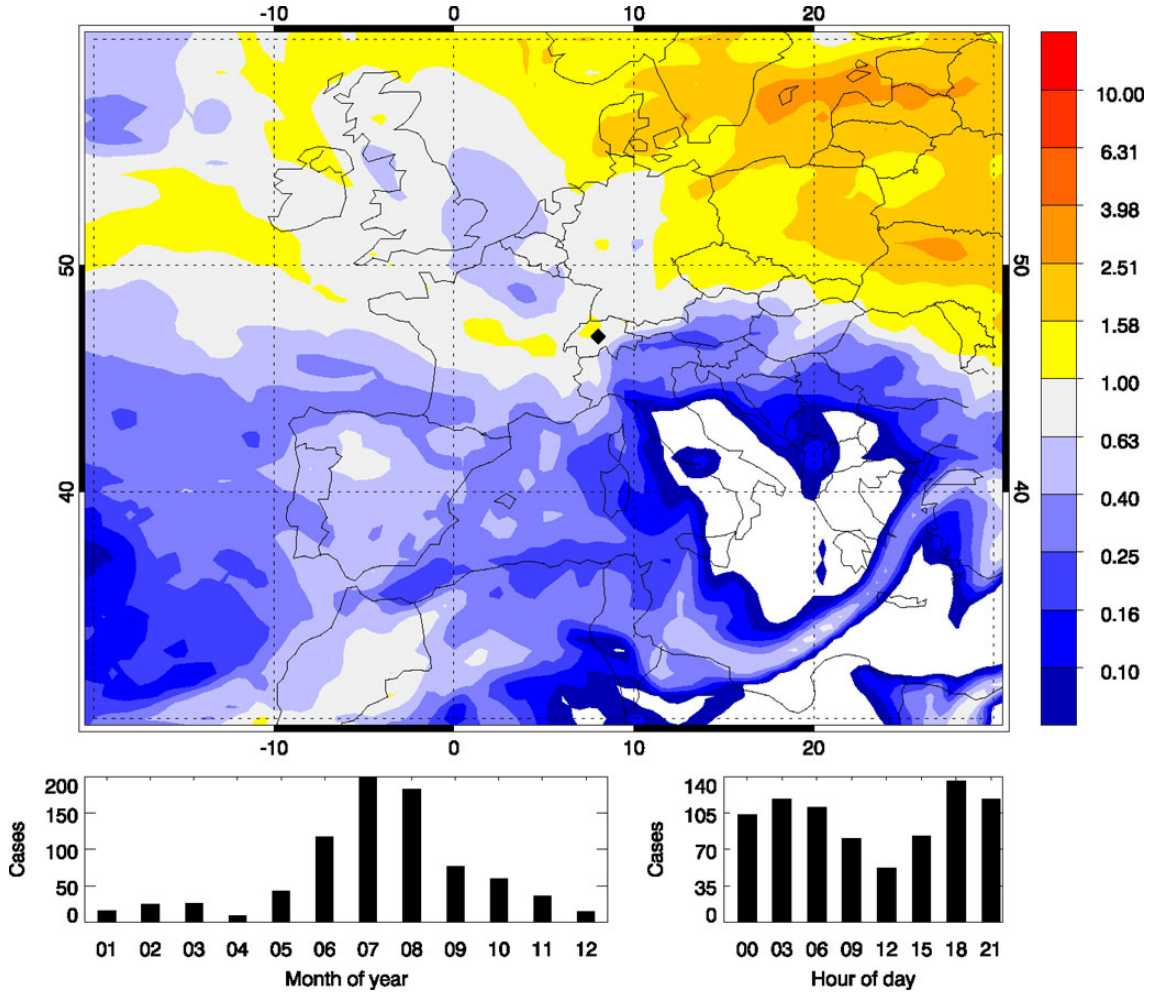

Fig. 13. Relative footprint map corresponding to low CO_2 but high APO and O_2 (subset 4). See Fig. 10 for further details

seasonal cycle observed at Jungfraujoch (Fig. 4). Note that there is a significant increase in O_2 as well as APO from June to August such that this delay would indeed lead to anomalously low APO making this option highly probable. Finally, option (iv) might be acting in parallel since dry summer soils consume more oxygen in order to oxidise soil organic material or released methane from wetlands than it is produced from photosynthesis (Pezeshki and Delaune, 2002; Cuna et al., 2008). Whether this option can play a major role is difficult to judge due to the sparse information about this process of soil oxidation.

4.2.4 Low CO_2 and high APO (subset 4)

As shown in Fig. 4, the average CO_2 background concentration decreases during summertime due to photosynthesis whereas the background O_2 increases (ocean outgassing, land and ocean biosphere contribution). The subset of points with low CO_2 and high APO would thus be consistent with air masses influenced by CO_2 uptake by the biosphere combined with increased ocean outgassing. The footprint map generated from this cluster (Fig. 13) indeed consists predominantly of summer events, but a high residence time over the the North Atlantic is not evident. Rather, these air masses tend to frequently originate from high latitudes with somewhat enhanced residence time over Scandinavia, the Baltic countries and the East Sea. The low CO_2 values are in line with the fact that these regions have comparatively low fossil fuel CO_2 emissions (see CO_2 emission map, Fig. 1) but significant plant/forest-covered areas. The reason for the enhanced APO in these air masses, however, is not clear and needs further investigation.

4.2.5 High APO (corresponding to high O_2) and normal CO_2 (subset 5)

The subset with regular CO_2 and high APO values (corresponding also to high O_2 values, subset 5) is associated with air masses advected from the Western North Atlantic Ocean, in particular during late autumn, winter into early

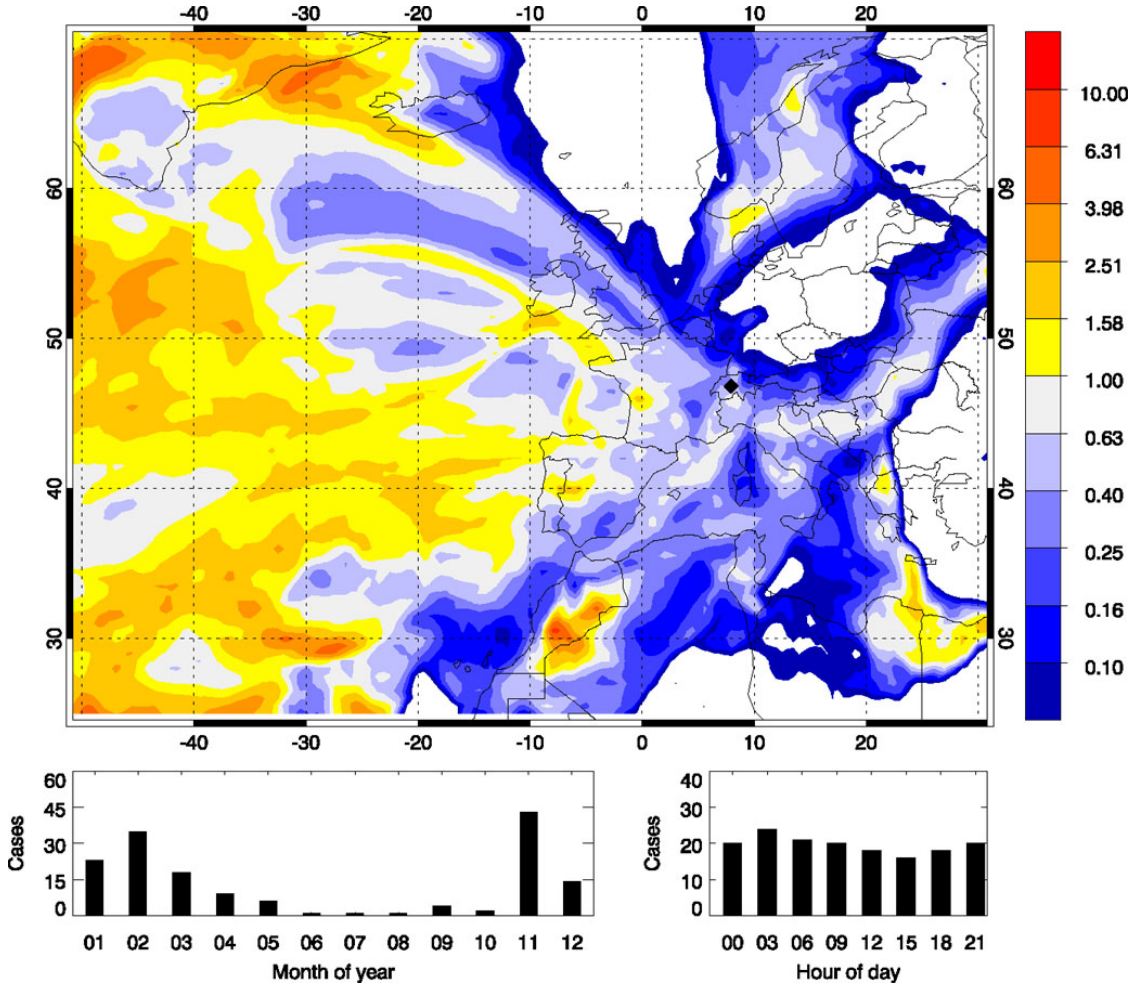

Fig. 14. Relative footprint map associated with high APO and also high O_2 (subset 5). See Fig. 10 for further details.

spring (from November to April). The corresponding relative footprint map is shown in Fig. 14. The main provenance of air masses is from the ocean, thus supporting the view of marine biospheric activity being responsible for high APO and oxygen concentrations measured at Jungfraujoch.

To support our view of marine air masses being responsible for high APO (and high O_2) concentrations at Jungfraujoch, we looked at the monthly maps of chlorophyll-*a* for the investigated period (January 2005–June 2009) available from the GlobColour project (http://www.globcolour.info/). The regions around Europe with highest marine photosynthesis rates are the Baltic Sea and the Atlantic Ocean in the vicinity of the coasts of Mauritania and Morocco. The maximum concentration of chlorophyll-*a* along the Western African coast is around 5–10 mg m^{-3} and occurs in general between February and April. Therefore, it can be argued that the high O_2 concentrations measured at Jungfraujoch could be influenced by the marine biospheric activity especially in the Atlantic Ocean and particularly in spring as shown in the footprint map.

4.2.6 Regular CO_2 and low APO (subset 6)

Most of the events associated with regular CO_2 and low O_2 (low APO) concentrations were observed in wintertime. The relative footprint map displayed in Fig. 15 shows a relative high residence time of air masses over the Mediterranean Sea and over Northern Africa. A possible mechanism for our observation could be an uptake of atmospheric oxygen by up-welling waters in the (Eastern) Mediterranean Sea under-saturated in oxygen (Kress and Herut, 2001). This is in line with a deepening of the thermocline during winter time bringing deeper waters to the surface. Indications that such O_2 uptake might be occurring at least periodically is given in a recent publication (Van Der Laan-Luijkx et al., 2010).

5 Conclusions

Continuous observations of carbon dioxide and oxygen concentrations at Jungfraujoch from 2005 to 2009 were combined with Lagrangian transport simulations to better

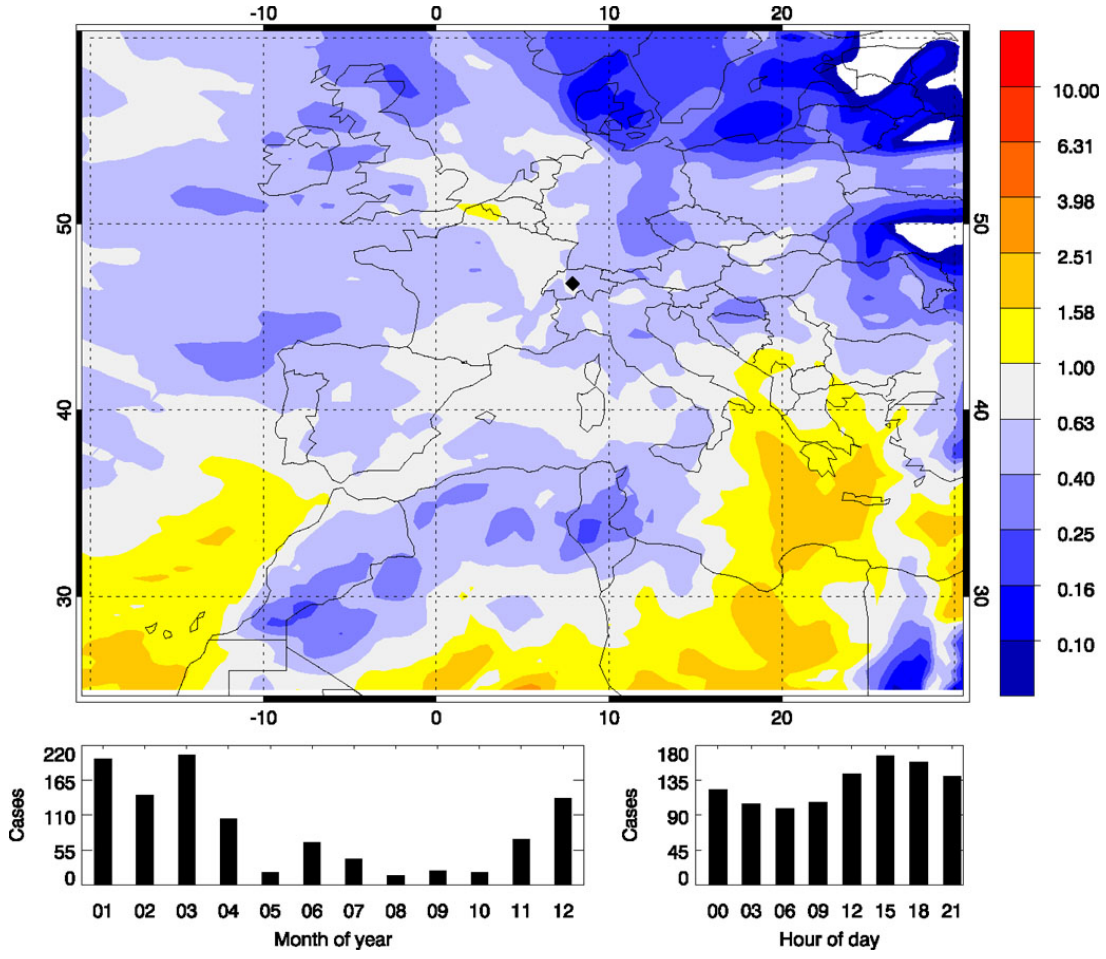

Fig. 15. Relative footprint map associated with regular CO_2 and low O_2 concentrations (subset 6). See Fig. 10 for further details.

understand the processes responsible for their variations and to identify main source and sink regions. For this purpose, footprints (maps of air residence time near the surface) were computed for each 3-hour measurement interval based on 5-days backward simulations using the Lagrangian particle dispersion model (LPDM) FLEXPART driven by meteorological data from ECMWF.

In general, footprints associated with particularly high CO_2 concentrations show transport of air masses from North Eastern Europe (Poland and Germany) or passing over densely populated and heavily industrialized areas like the Ruhr area in Germany and the Po Valley in Northern Italy. Transport from the Po Valley is mainly connected to south Foehn events. A detailed footprint analysis of clustered background corrected CO_2 and APO values was performed in order to trace source and sink areas as well as underlying processes resonsible for observed short-term variations. A selection of six clusters based on a scatter-plot of APO versus CO_2 allowed not only a spatial distinction (major source and sink areas) but also seasonal differentiation (winter, summer). Short-term variations with low CO_2 values, occuring in spring and summer, exhibit clearer characteristics than those with medium or high CO_2 (autumn, winter and spring). Additional work is needed to fully understand this results. Finally, this study demonstrates the great use of LPDM simulations to support the classification of air masses and to explain short-term fluctuations in the CO_2 and O_2 observation records. The addition of more atmospheric trace gases, such N_2O, CO and CH_4 would further constrain the influence of air mass transport on measured concentrations. In future studies it would also be desirable to use wind fields at even higher resolution than used here to better resolve the flow pattern over the complex topography of the Alps.

Acknowledgements. This work was mainly performed within the scope of the AEROCARB project funded under the EU Framework V programme Contract No. EVK2-1999-00013 and was continued within CarboEurope-IP. The Swiss contribution to both projects was financed by the Swiss State Secretariat for Education and Research SER. It was also supported by the Swiss National Science Foundation as well as the Swiss GCOS office. We are grateful to the International Foundation High Altitude Research

Stations Jungfraujoch and Gornergrat for supporting our research, in particular we are thankful to the custodians at Jungfraujoch who took the flask samples and were looking after the online instrument.

Edited by: M. Heimann

References

Bader, S. and Croci-Maspoli, M.: The weather in 2007, International Foundation HFSJG, Activity Report 2007, MeteoSchweiz, Bundesamt für Meteorologie und Klimatologie, Zürich, 6, 2007.

Bader, S. and Schlegel, T.: The weather in 2005, International Foundation HFSJG, Activity Report 2005, MeteoSchweiz, Bundesamt für Meteorologie und Klimatologie, Zürich, 8, 2005.

Baltensperger, U., Gäggeler, H. W., Jost, D. T., and Emmenegger, M.: Continuous background aerosol monitoring with the epiphaniometer, Atmos. Environ., 25, 629–634, 1991.

Balzani Lööv, J. M. B., Henne, S., Legreid, G., Staehelin, J., Reimann, S., Prevot, A. S. H., Steinbacher, M., and Vollmer, M. K.: Estimation of background concentrations of trace gases at the Swiss Alpine site Jungfraujoch (3580 m a.s.l.), J. Geophys. Res.-Atmos., 113, D22305, doi:10.1029/2007JD009751, 2008.

Battle, M., Bender, M. L., Tans, P. P., White, J. W. C., Ellis, J. T., Conway, T., and Francey, R. J.: Global carbon sinks and their variability inferred from atmospheric O_2 and $\delta^{13}C$, Science, 287, 2467–2470, 2000.

Bender, M., Ellis, T., Tans, P., Francey, R., and Lowe, D.: Variability in the O_2/N_2 ratio of Southern Hemisphere air, 1991–1994: implications for the carbon cycle, Global Biogeochem. Cy., 10, 9–21, 1996.

Bender, M. L., Ho, D. T., Hendricks, M. B., Mika, R., Battle, M. O., Tans, P. P., Conway, T. J., Sturtevant, B., and Cassar, N.: Atmospheric O_2/N_2 changes, 1993–2002: implications for the partitioning of fossil fuel CO_2 sequestration, Global Biogeochem. Cy., 19, GB4017, doi:10.1029/2004GB002410, 2005.

Campana, M., Li, Y. S., Staehelin, J., Prevot, A. S. H., Bonasoni, P., Loetscher, H., and Peter, T.: The influence of south foehn on the ozone mixing ratios at the high alpine site Arosa, Atmos. Environ., 39, 2945–2955, 2005.

Castro, L. M., Pio, C. A., Harrison, R. M., and Smith, D. J. T.: Carbonaceous aerosol in urban and rural European atmospheres: estimation of secondary organic carbon concentrations, Atmos. Environ., 33, 2771–2781, 1999.

Collaud Coen, M., Weingartner, E., Schaub, D., Hueglin, C., Corrigan, C., Henning, S., Schwikowski, M., and Baltensperger, U.: Saharan dust events at the Jungfraujoch: detection by wavelength dependence of the single scattering albedo and first climatology analysis, Atmos. Chem. Phys., 4, 2465–2480, doi:10.5194/acp-4-2465-2004, 2004.

Cozic, J., Verheggen, B., Mertes, S., Connolly, P., Bower, K., Petzold, A., Baltensperger, U., and Weingartner, E.: Scavenging of black carbon in mixed phase clouds at the high alpine site Jungfraujoch, Atmos. Chem. Phys., 7, 1797–1807, doi:10.5194/acp-7-1797-2007, 2007.

Cozic, J., Verheggen, B., Weingartner, E., Crosier, J., Bower, K. N., Flynn, M., Coe, H., Henning, S., Steinbacher, M., Henne, S., Collaud Coen, M., Petzold, A., and Baltensperger, U.: Chemical composition of free tropospheric aerosol for PM1 and coarse mode at the high alpine site Jungfraujoch, Atmos. Chem. Phys., 8, 407–423, doi:10.5194/acp-8-407-2008, 2008.

Cui, J., Sprenger, M., Staehelin, J., Siegrist, A., Kunz, M., Henne, S., and Steinbacher, M.: Impact of stratospheric intrusions and tercontinental transport on ozone at Jungfraujoch in 2005: comparison and validation of two Lagrangian approaches, Atmos. Chem. Phys., 9, 3371–3383, doi:10.5194/acp-9-3371-2009, 2009.

Cuna, S., Pendall, E., Miller, J. B., Tans, P. P., Dlugokencky, E., and White, J. W. C.: Separating contributions from natural and anthropogenic sources in atmospheric methane from the Black Sea region, Romania, Appl. Geochem., 23, 2871–2879, 2008.

Folini, D., Ubl, S., and Kaufmann, P.: Lagrangian particle dispersion modeling for the high Alpine site Jungfraujoch. J. Geophys. Res., 113, D18111, doi:10.1029/2007JD009558, 2008.

Forrer, J., Ruttimann, R., Schneiter, D., Fischer, A., Buchmann, B., and Hofer, P.: Variability of trace gases at the high-Alpine site Jungfraujoch caused by meteorological transport processes, J. Geophys. Res.-Atmos., 105, 12241–12251, 2000.

Forster, P., Ramaswamy, V., Artaxo, P., Berntsen, T., Betts, R., Fahey, D. W., Haywood, J., Lean, J., Lowe, D. G., Myhre, G., Nganga, J., Prinn, R., Raga, G., Schulz, M., and Van Dorland, R.: Changes in Atmospheric Constituents and in Radiative Forcing., Climate Change 2007: The Physical Science Basis. Contribution of Working Group I to the Fourth Assessment Report of the Intergovernmental Panel on Climate Change, edited by: Solomon, S., Qin, D., Manning, M., Chen, Z., Marquis, M., Averyt, K. B., Tignor, M., and Miller, H. L., Cambridge University Press, Cambridge, UK and New York, NY, USA, 106 pp., 2007.

Gurk, Ch., Fischer, H., Hoor, P., Lawrence, M. G., Lelieveld, J., and Wernli, H.: Airborne in-situ measurements of vertical, seasonal and latitudinal distributions of carbon dioxide over Europe, Atmos. Chem. Phys., 8, 6395–6403, doi:10.5194/acp-8-6395-2008, 2008.

Henne, S., Dommen, J., Neininger, B., Reimann, S., Staehelin, J., and Prevot, A. S. H.: Influence of mountain venting in the Alps on the ozone chemistry of the lower free troposphere and the European pollution export, J. Geophys. Res.-Atmos., 110, D22307 doi:10.1029/2005JD005936, 2005a.

Henne, S., Furger, M., and Prevot, A. S. H.: Climatology of mountain venting-induced elevated moisture layers in the lee of the Alps, J. Appl. Meteorol., 44, 620–633, 2005b.

Henne, S., Klausen, J., Junkermann, W., Kariuki, J. M., Aseyo, J. O., and Buchmann, B.: Representativeness and climatology of carbon monoxide and ozone at the global GAW station Mt. Kenya in equatorial Africa, Atmos. Chem. Phys., 8, 3119–3139, doi:10.5194/acp-8-3119-2008, 2008.

Hirdman, D., Burkhart, J. F., Sodemann, H., Eckhardt, S., Jefferson, A., Quinn, P. K., Sharma, S., Strm, J., and Stohl, A.: Long-term trends of black carbon and sulphate aerosol in the Arctic: changes in atmospheric transport and source region emissions, Atmos. Chem. Phys., 10, 9351–9368, doi:10.5194/acp-10-9351-2010, 2010.

Ishidoya, S., Morimoto, S., Sugawara, S., Watai, T., Machida, T., Aoki, S., Nakazawa, T., and Yamanouchi, T.: Gravitational separation suggested by O_2/N_2, $\delta^{15}N$ of N_2, $\delta^{18}O$ of O_2, Ar/N_2 observed in the lowermost part of the stratosphere at northern middle and high latitudes in the early spring of 2002, Geophys.

Res. Lett., 35, L03812, doi:10.1029/2007GL031526, 2008.

Kaiser, A., Scheifinger, H., Spang,l W., Weiss, A., Gilge, S., Fricke, W., Ries, L., Cemas, D., and Jesenovec, B.: Transport of nitrogen oxides, carbon monoxide and ozone to the Alpine Global Atmosphere Watch stations Jungfraujoch (Switzerland), Zugspitze and Hohenpeissenberg (Germany), Sonnblick (Austria) and Mt. Krvavec (Slovenia), Atmos. Environ.t, 41(40), 9273–9287, 2007.

Keeling, R. F.: Measuring correlations between atmospheric oxygen and carbon-dioxide mole fractions – a preliminary-study in urban air, J. Atmos. Chem., 7, 153–176, 1988.

Keeling, R. F. and Shertz, S. R.: Seasonal and Interannual Variations in Atmospheric Oxygen and Implications for the Global Carbon Cycle, Nature, 358, 723–727, 1992.

Keeling, R. F., Najjar, R. P., Bender, M. L., and Tans, P. P.: What atmospheric oxygen measurements can tell us about the global carbon-cycle, Global Biogeochem. Cy., 7, 37–67, 1993.

Keeling, R. F., Manning, A. C., McEvoy, E. M., and S. R. Shertz, S. R.: Methods for measuring changes in atmospheric O_2 concentration and their application in Southern Hemisphere air, J. Geophys. Res., 103, 3381–3397, 1998.

Keeling, R. F., Blaine, T., Paplawsky, B., Katz, L., Atwood, C., and Brockwell, T.: Measurement of changes in atmospheric Ar/N_2 ratio using a rapid-switching, single-capillary mass spectrometer system, Tellus B, 56, 322–338, 2004.

Keeling, R. F., Manning, A. C., Paplawsky, B., and Cox, A.: On the long-term stability of O_2/N_2 reference gases, in: Proc. 12th WMO/IAEA Meeting of Experts on Carbon Dioxide Concentration and Related Tracers Measurement Techniques, WMO Tech. Doc. 1275, Toronto, ON, Canada, WMO 131–140, 2005.

Kozlova, E. A., Manning, A. C., Kisilyakhov, Y., Seifert, T., and Heimann, M.: Seasonal, synoptic, and diurnal-scale variability of biogeochemical trace gases and O_2 from a 300-m tall tower in Central Siberia, Global Biogeochem. Cy., 22, GB4020, doi:10.1029/2008GB003209, 2008.

Kress, N. and Herut, B.: Deep Sea Research Part I, Oceanogr. Res. Pap., 48, 2347–2372, 2001.

Langenfelds, R. L., van der Schoot, M. V., Francey, R. J., Steele, L. P., Schmidt, M., and Mukai, H.: Modification of air standard composition by diffusive and surface processes., J. Geophys. Res., 110, D13307, doi:10.1029/2004JD005482, 2005.

Lanz, V. A., Henne, S., Staehelin, J., Hueglin, C., Vollmer, M. K., Steinbacher, M., Buchmann, B., and Reimann, S.: Statistical analysis of anthropogenic non-methane VOC variability at a European background location (Jungfraujoch, Switzerland), Atmos. Chem. Phys., 9, 3445–3459, doi:10.5194/acp-9-3445-2009, 2009.

Lewis, A. C., Evans, M. J., Methven, J., Watson, N., Lee, J. D., Hopkins, J. R., Purvis, R. M., Arnold, S. R., McQuaid, J. B., Whalley, L. K., Pilling, M. J., Heard, D. E., Monks, P. S., Parker, A. E., Reeves, C. E., Oram, D. E., Mills, G., Bandy, B. J., Stewart, D., Coe, H., Williams, P., and Crosier, J.: Chemical composition observed over the mid-Atlantic and the detection of pollution signatures far from source regions, J. Geophys. Res., 112, D10S39, doi:10.1029/2006JD007584, 2007.

Li, Y. S., Campana, M., Reimann, S., Schaub, D., Stemmler, K., Staehelin, J., and Thomas, P. T.: Hydrocarbon concentrations at the Alpine mountain sites Jungfraujoch and Arosa, Atmos. Environ., 39, 1113–1127, 2005.

Lin, C., Brunner, D., and Gerbig, C.: Studying atmospheric transport through Lagrangian models, Eos. Trans. Am., 92(21), 177-178, 2011.

Lugauer, M., Baltensperger, U., Furger, M., Gaggeler, H. W., Jost, D. T., Schwikowski, M., and Wanner, H.: Aerosol transport to the high Alpine sites Jungfraujoch (3454 m a.s.l.) and Colle Gnifetti (4452 m a.s.l.), Tellus B, 50, 76–92, 1998.

Manning, A. C.: Temporal variability of atmospheric oxygen from both continuous measurements and a flask sampling network: tools for studying the global carbon cycle, Ph.D. thesis, University of California, San Diego, California, USA, 2001.

Manning, A. C. and Keeling, R. F.: Global oceanic and land biotic carbon sinks from the Scripps atmospheric oxygen flask sampling network, Tellus B, 58, 95–116, 2006.

Marland, G., Boden, T. A., and Andres, R. J.: Global, Regional, and National Fossil-Fuel CO_2 Emissions. In Trends: A Compendium of Data on Global Change. Carbon Dioxide Information Analysis Center, Oak Ridge National Laboratory, US Department of Energy, Oak Ridge, Tenn., USA, 2009.

Moody, J. L. and Galloway, J. N.: Quantifying the relationship between atmospheric transport and the chemical composition of precipitation on Bermuda, Tellus B, 40(5), 463–479, 1988.

Morimoto, S., Nakazawa, T., Aoki, S., Hashida, G., and Yamanouchi, T.: Concentration variations of atmospheric CO_2 observed at Syowa Station, Antarctica from 1984 to 2000, Tellus B, 55, 170–177, 2003.

Nakazawa, T., Ishizawa, M., Higuchi, K., and Trivett, N. B. A.: Two curve fitting methods applied to CO_2 flask data, Environmetrics, 8(3), 197–218, 1997.

Paris, J.-D., Stohl, A., Ciais, P., Ndlec, P., Belan, B. D., Arshinov, M. Yu., and Ramonet, M.: Sourcereceptor relationships for airborne measurements of CO_2, CO and O_3 above Siberia: a cluster-based approach, Atmos. Chem. Phys., 10, 1671–1687, doi:10.5194/acp-10-1671-2010, 2010.

Petzold, A., Weinzierl, B., Huntrieser, H., Stohl, A., Real, E., Cozic, J., Fiebig, M., Hendricks, J., Lauer, A., Law, K., Roiger, A., Schlager, H., and Weingartner, E.: Perturbation of the European free troposphere aerosol by North American forest fire plumes during the ICARTT-ITOP experiment in summer 2004, Atmos. Chem. Phys., 7, 5105–5127, doi:10.5194/acp-7-5105-2007, 2007.

Pezeshki, S. R. and DeLaune, R. D.: Effects of soil oxidation-reduction conditions on internal oxygen transport, root aeration, and growth of wetland plants, Proceedings of a conference on sustainability of wetlands and water resources: how well can riverine wetlands continue to support society into the 21st century?, Gen. Tech. Rep. SRS-50. Asheville, NC:US Department of Agriculture, Forest Service, Southern Research Station, 2002.

Popa, M. E., Gloor, M., Manning, A. C., Jordan, A., Schultz, U., Haensel, F., Seifert, T., and Heimann, M.: Measurements of greenhouse gases and related tracers at Bialystok tall tower station in Poland, Atmos. Meas. Tech., 3, 407–427, doi:10.5194/amt-3-407-2010, 2010.

Reimann, S., Schaub, D., Stemmler, K., Folini, D., Hill, M., Hofer, P., and Buchmann, B.: Halogenated greenhouse gases at the Swiss High Alpine Site of Jungfraujoch (3580 m a.s.l.): Continuous measurements and their use for regional

European source allocation, J. Geophys. Res., 109, D05307, doi:10.1029/2003JD003923, 2004.

Reimann, S., Vollmer, M. K., Folini, D., Steinbacher, M., Hill, M., Buchmann, B., Zander, R., and Mahieu, E.: Observations of long-lived anthropogenic halocarbons at the high-Alpine site of Jungfraujoch (Switzerland) for assessment of trends and European sources, Sci. Total Environ., 391, 224–231, 2008.

Rotty, R. M.: Estimates of seasonal variation in fossil fuel CO_2 emissions, Tellus B, 39, 184–202, 1987.

Sabine, C. L., Feely, R. A., Gruber, N., Key, R. M., Lee, K., Bullister, J. L., Wanninkhof, R., Wong, C. S., Wallace, D. W. R., Tilbrook, B., Millero, F. J., Peng, T. H., Kozyr, A., Ono, T., and Rios, A. F.: The oceanic sink for anthropogenic CO_2, Science, 305(5682), 367–371, 2004.

Scheifinger, H. and Kaiser, A.: Validation of trajectory statistical methods, Atmos. Environ., 41, 8846–8856, 2007.

Schulze, E. D., Luyssaert, S., Ciais, P. A. F., Janssens, I. A., Soussana, J. F., Smith, P., Grace, J., Levin, I., Thiruchittampalam, B., Heimann, M., Dolman, A. J., Valentini, R., Bousquet, P., Peylin, P., Peters, W., Rödenbeck, C., Etiope, G., Vuichard, N., Wattenbach, M., Nabuurs, G. J., Poussi, Z., Nieschulze, J., Gash, J. H., and CarboEurope Team: Europe's Greenhouse-Gas Balance: Methane and nitrous oxide emissions compensate CO_2 sinks, Nat. Geosci., 2, 842–850, 2009.

Schwikowski, M., Seibert, P., Baltensperger, U., and Gaggeler, H. W.: A Study of an Outstanding Saharan Dust Event at the High Alpine Site Jungfraujoch, Switzerland, Atmos. Environ., 29, 1829–1842, 1995.

Seibert, P.: South foehn studies since the Alpex experiment, Meteorol. Atmos. Phys., 43, 91–103, 1990.

Seibert, P. and Frank, A.: Source-receptor matrix calculation with a Lagrangian particle dispersion model in backward mode, Atmos. Chem. Phys., 4, 51–63, doi:10.5194/acp-4-51-2004, 2004.

Seibert, P., Kromp-Kolb, H., Baltensperger, U., Jost, D. T., Schwikowski, M., Kasper, A., and Puxbaum, H.: Trajectory analysis of aerosol measurements at high alpine sites, Proceedings of the EUROTRAC Symposium '94 SPB Academic Publishing, Hague, edited by: Borrell, P. M., Borrell, P., Cvitas, T., and Seiler, W., 1283 pp., 689–693, 1994.

Seibert, P., Kromp-Kolb, H., Kasper, A., Kalina, M., Puxbaum, H., Jost, D. T., Schwikowski, M., and Baltensperger, U.: Transport of polluted boundary layer air from the Po Valley to high alpine sites, Atmos. Environ., 32, 3953–3965, 1998.

Severinghaus, J. P.: Studies of the terrestrial O_2 and carbon cycle in sand dunes gases and in biosphere PhD thesis, Columbia University, New York, USA, 1995.

Siegel, D. A., Doney, S. C., and Yoder, J. A.: The North Atlantic spring phytoplankton bloom and Sverdrup's critical depth hypothesis, Science, 296, 730–733, 2002.

Stephens, B. B., Keeling, R. F., Heimann, M., Six, K. D., Munane, R., and Caldeira, K.: Testing global ocean carbon cycle models using measurements of atmospheric O_2 and CO_2 concentration, Global Biogeochem. Cy., 12, 213–230, 1998.

Stoffyn, E. P., Potter, T. M., Leonard, J. D., and Pocklington, R.: The identification of black carbon particles with the analytical scanning electron microscope: methods and initial results, Sci. Total Environ., 198, 211–223, 1997.

Stohl, A.: The FLEXTRA and FLEXTRAPART homepage: http://zardoz.nilu.no/~andreas/flextra+flexpart.html, 2006.

Stohl, A. and Seibert, P.: Accuracy of trajectories as determined from the conservation of meteorological tracers, Q. J. Roy. Meteorol. Soc., 124, 1465–1484, 1998.

Stohl, A., Wotawa, G., Seibert, P., and Kromp-Kolb, H.: Interpolation errors in wind fields as a function of spatial and temporal resolution and their impact on different types of kinematic trajectories, J. Appl. Meteor., 34, 2149–2165, 1995.

Stohl, A., Haimberger, L., Scheele, M. P., and Wernli, H.: An intercomparison of results from three trajectory models, Meteorol. Appl., 8, 127–135, 1999.

Stohl, A., Forster, C., Frank, A., Seibert, P., and Wotawa, G.: Technical note: The Lagrangian particle dispersion model FLEXPART version 6.2, Atmos. Chem. Phys., 5, 2461–2474, doi:10.5194/acp-5-2461-2005, 2005.

Sturm, P.: Atmospheric oxygen and associated tracers from flask sampling and continuous measurements: tools for studying the global carbon cycle, Ph.D. thesis, University of Bern, Bern, Switzerland, 2005.

Sverdrup, H. U.: On conditions for the vernal blooming of phytoplankton, J. Conseil/Conseil International pour P Exploration de la Mer, 18, 287–295, 1953.

Takahashi, T., Broecker, W. S., and Langer, S.: Redfield ratio based on chemical data from isopycnal surfaces, J. Geophys. Res., 90, 6907– 6924, 1985.

Thompson, R. L., Manning, A. C., Gloor, E., Schultz, U., Seifert, T., Hänsel, F., Jordan, A., and Heimann, M.: In-situ measurements of oxygen, carbon monoxide and greenhouse gases from Ochsenkopf tall tower in Germany, Atmos. Meas. Tech., 2, 573–591, doi:10.5194/amt-2-573-2009, 2009.

Tohjima, Y., Mukai, H., Nojiri, Y., Yamagishi, H., and Machida, T.: Atmospheric O_2/N_2 measurements at two Japanese sites: estimation of global oceanic and land biotic carbon sinks and analysis of the variations in atmospheric potential oxygen (APO), Tellus B, 60, 213–225, 2008.

Tuzson, B., Henne, S., Brunner, D., Steinbacher, M., Mohn, J., Buchmann, B., and Emmenegger, L.: Continuous isotopic composition measurements of tropospheric CO_2 at Jungfraujoch (3580 m a.s.l.), Switzerland: real-time observation of regional pollution events, Atmos. Chem. Phys., 11, 1685–1696, doi:10.5194/acp-11-1685-2011, 2011.

Uglietti, C., Leuenberger, M., and Valentino, F. L.: Comparison between real time and flask measurements of atmospheric O_2 and CO_2 performed at the High Altitude Research Station Jungfraujoch, Switzerland, Sci. Total Environ., 391, 196–202, 2008.

Uglietti, C., Leuenberger, M., and Brunner, D.: Large-scale European source and flow patterns retrieved from back-trajectory interpretations of CO_2 at the high alpine research station Jungfraujoch, Atmos. Chem. Phys. Discuss., 11, 813–857, doi:10.5194/acpd-11-813-2011, 2011.

Valentino, F. L., Leuenberger, M., Nyfeler, P., Moret, H. P., Sturm, P., Slemr, F., and Brenninkmeijer, C. A. M.: Description of an airborne instrument for continuous O_2 and CO_2 analysis, Environ. Sci. Technol., 2007.

Valentino, F. L., Leuenberger, M., Uglietti, C., and Sturm, P.: Measurements and trend analysis of O_2, CO_2 and $\delta^{13}C$ of CO_2 from the high altitude research station Junfgraujoch, Switzerland – a comparison with the observations from the remote site Puy de Dome, France, Sci. Total Environ., 391, 203–210, 2008.

van der Laan-Luijkx, I. T., Neubert, R. E. M., van der Laan, S., and Meijer, H. A. J.: Continuous measurements of atmospheric oxygen and carbon dioxide on a North Sea gas platform, Atmos. Meas. Tech., 3, 113–125, doi:10.5194/amt-3-113-2010, 2010.

Weingartner, E., Nyeki, S., and Baltensperger, U.: Seasonal and diurnal variation of aerosol size distributions ($10 < D < 750$ nm) at a high-alpine site (Jungfraujoch 3580 m a.s.l.), J. Geophys. Res.-Atmos., 104, 26809–26820, 1999.

Zeng, Y. and Hopke, P. K.: A study of the sources of acid precipitation in Ontario, Canada, Atmos. Environ., 23, 1499–1509, 1989.